medRxiv preprint doi: https://doi.org/10.1101/2020.12.09.20246389; this version posted December 11, 2020. The copyright holder for this preprint **(which was not certified by peer review)** is the author/funder, who has granted medRxiv a license to display the preprint in perpetuity.

It is made available under a CC-BY-ND 4.0 International license .

Untargeted metabolomics of COVID-19 patient serum reveals potential prognostic markers of both severity and outcome.

Ivayla Roberts[1,*], Marina Wright Muelas[1,*†], Joseph M. Taylor[2,*], Andrew S. Davison[2,*], Yun Xu[1,*], Justine M. Grixti[1,*], Nigel Gotts[1,*], Anatolii Sorokin[1], Royston Goodacre[1], Douglas B. Kell[1,3†]

[1]Department of Biochemistry and Systems Biology, Institute of Systems, Molecular and Integrative Biology, University of Liverpool, UK

[2]Department of Clinical Biochemistry and Metabolic Medicine, Liverpool Clinical Laboratories, Royal Liverpool University Hospitals Trust, Liverpool, UK.

[3]Novo Nordisk Foundation Centre for Biosustainability, Technical University of Denmark, Building 220, Chemitorvet, Kgs Lyngby 2000, Denmark.

*Equal contributions

†Corresponding authors Dr. Marina Wright Muelas (m.wright-muelas@liverpool.ac.uk), Prof. Douglas B. Kell (douglas.kell@liverpool.ac.uk)

Abstract

The diagnosis of COVID-19 is normally based on the qualitative detection of viral nucleic acid sequences. Properties of the host response are not measured but are key in determining outcome. Although metabolic profiles are well suited to capture host state, existing metabolomics studies are either underpowered, measure only a restricted subset of metabolites ('targeted metabolomics'), compare infected individuals against uninfected control cohorts that are not suitably matched, or do not provide a compact predictive model.

We here provide a well-powered, untargeted metabolomics assessment of 120 COVID-19 patient samples acquired at hospital admission. The study aims to predict patient's infection severity (i.e. mild or severe) and potential outcome (i.e. discharged or deceased).

High resolution untargeted LC-MS/MS analysis was performed on patient serum using both positive and negative ionization. A subset of 20 intermediary metabolites predictive of severity or outcome were selected based on univariate statistical significance and a multiple predictor Bayesian logistic regression model. The predictors were selected for their relevant biological function and include cytosine (reflecting viral load), kynurenine (reflecting host inflammatory response), nicotinuric acid, and multiple short chain acylcarnitines (energy metabolism) among others.

Currently, this approach predicts outcome and severity with a Monte Carlo cross validated area under the ROC curve of 0.792 (SD 0.09) and 0.793 (SD 0.08), respectively. Prognostic tests based on the markers discussed in this paper could allow improvement in the planning of COVID-19 patient treatment.

Key words: COVID-19, serum, untargeted metabolomics, LC-MS/MS, Orbitrap

NOTE: This preprint reports new research that has not been certified by peer review and should not be used to guide clinical practice.

medRxiv preprint doi: https://doi.org/10.1101/2020.12.09.20246389; this version posted December 11, 2020. The copyright holder for this preprint **(which was not certified by peer review)** is the author/funder, who has granted medRxiv a license to display the preprint in perpetuity.

It is made available under a CC-BY-ND 4.0 International license .

Abbreviations:

AEX-LC-MS/MS	anion-exchange LC-MS	**LC-MS**	liquid chromatography mass spectrometry
AF	atrial fibrillation	**LC-MS/MS**	liquid chromatography tandem mass spectrometry
ALT	alanine aminotransferase	**LFC**	log fold change
ARDS	acute respiratory distress syndrome	**Lymphs**	lymphocyte count
AUC	area under the curve	**MB-PCA**	multiblock PCA
BMI	body mass index	**MSI**	metabolomics Standards Initiative
BP	systolic blood pressure	**MSML**	mass spectrometry metabolite library
CI	confidence interval	**NEWS**	national early warning score
COVID-19	Coronavirus disease 2019	**NICE**	national institute for health and care excellence
CPAP	continuous positive airway pressure	**NMR**	nuclear magnetic resonance
CRP	C-reactive protein	**OR**	odds ratio
CRS	cytokine release storms	**PCA**	principal component analysis
CV	coefficient of variation	**PCR**	polymerase chain reaction
eGFR	estimated glomerular filtration rate	**PLTs**	platelets count
ESI	electrospray ionization	**QC**	quality control
FC	fold change	**RLUH**	royal Liverpool university hospital
FDR	false discovery rate	**ROC**	receiver operating characteristic
FIO_2	fraction of inspired oxygen	**rRNA**	ribosomal RNA
GC-MS	gas chromatography mass spectrometry	**RT**	retention time
GCS	Glasgow coma scale	**RTPCR**	reverse transcription PCR
GLM	generalized linear models	**SARS-CoV-2**	severe acute respiratory syndrome coronavirus-2
Hb	haemoglobin levels	**SD**	standard deviation
HCT	hematocrit	**SOB**	shortness of breath
IHD	ischaemic heart disease	**WBC**	white blood cell count
IQA	inter-batch quality assurance		

medRxiv preprint doi: https://doi.org/10.1101/2020.12.09.20246389; this version posted December 11, 2020. The copyright holder for this preprint **(which was not certified by peer review)** is the author/funder, who has granted medRxiv a license to display the preprint in perpetuity.

It is made available under a CC-BY-ND 4.0 International license .

Contents

Abstract 1
Introduction 4
Results 6
Exploratory analysis 6
Predictive models 6
Metabolic pathways linked to severity and outcome 9
Elevated serum cytosine association with severity and outcome 9
Tryptophan and kynurenine metabolism compounds associate with both severity and outcome 10
Beta oxidation metabolites, acylcarnitines, increased in severe and deceased outcome patients 11
Other compounds 11
Model compounds adjusted for demographic factors and underlying conditions 11
Discussion 12
Alterations in pyrimidine metabolites predictive of severity and outcome 14
Tryptophan - kynurenine degradation 14
Beta oxidation 15
Compounds requiring further investigation 15
Limitations and future work 16
Conclusions 16
Methods 17
Sample acquisition 17
Sample preparation for metabolomics analysis 18
LC-MS /MS analysis of spent serum samples 19
LC-MS/MS data preprocessing and analysis 19
Area normalization and batch correction 19
Metadata and multiblock analysis 20
Selection of significant metabolic features 20
Signal curation 20
Pathway enrichment analysis 20
Multiple predictor models 21
Adjusted compounds significance 21
Acknowledgements 22
Contributions 22
Conflict of interest 22
References 23

medRxiv preprint doi: https://doi.org/10.1101/2020.12.09.20246389; this version posted December 11, 2020. The copyright holder for this preprint **(which was not certified by peer review)** is the author/funder, who has granted medRxiv a license to display the preprint in perpetuity.

It is made available under a CC-BY-ND 4.0 International license .

Introduction

The severe acute respiratory syndrome coronavirus-2 (SARS-CoV-2) outbreak started in Wuhan, China, in 2019, and quickly resulted in a worldwide pandemic, challenging healthcare systems with the need to provide intensive care to a previously inconceivable number of patients (Bennet et al., 2020). SARS-CoV-2 presents with a wide range of symptoms, ranging from minor, unspecific ones, including anosmia, a dry persistent cough, fever, diarrhoea, in certain cases combined with mild pneumonia, to more severe, potentially life-threatening symptoms, such as severe pneumonia with dyspnoea, tachypnoea and disturbed gas exchange. Approximately 5% of severely infected patients develop lung dysfunction, requiring ventilation, and shock or multiple organ failure (Marietta et al., 2020; Wu and McGoogan, 2020). In some cases, symptoms remain for an extended period ('long COVID').

The reasons behind the wide variability in individual responses to COVID-19, i.e. the illness resulting from SARS-CoV-2 infection, are still poorly understood, though some appear to involve interferon responses (Arunachalam et al., 2020; Hadjadj et al., 2020; Zhang et al., 2020). Much research, and evidence from the clinic, points towards the idea that severe complications in COVID-19 arise through a vasculopathy and coagulopathy elicited by infection rather than via the typical inflammatory responses normally observed in acute respiratory distress syndrome or cytokine release storms (Fox et al., 2020; Grobler et al., 2020; Leisman et al., 2020; Libby and Lüscher, 2020; Paranjpe et al., 2020; Pretorius et al., 2020; Zheng et al., 2020). Prognostic scores attempt to transform complex clinical pictures into tangible numerical values. However, many of these novel COVID-19 prognostic scores have been found to have a high risk of bias, possibly reflecting the fact that they have been developed in small cohorts, and many have been published without clear details of model derivation and testing (Knight et al., 2020; Wynants et al., 2020).

Understanding changes in the biochemistry of an individual who is ostensibly healthy (Dunn et al., 2011; Dunn et al., 2015), including when they may show no overt symptoms of infection with SARS-CoV-2, remains a huge challenge. Similar questions apply to understanding who is likely to survive (unaided or via intervention) and who is likely to die from COVID-19 once diagnosed.

For fundamental reasons, the metabolome is a more sensitive indicator of the biochemical status of a cell or organism than is a proteome or a transcriptome (Kell and Oliver, 2016; Oliver et al., 1998; Raamsdonk et al., 2001). Consequently, metabolomic analyses of patient samples promise to enable understanding of biochemical changes in relation to poorly understood processes, for instance as recently shown in human frailty in ageing populations (Rattray et al., 2019). Because they measure the effects on the host and not simply the presence of the infecting agent, such metabolomic studies could provide a set of markers that can be of significant use for rapid tests, complementary to current polymerase chain reaction (PCR) or antibody tests, for confirmation of SARS-CoV-2 infection, disease severity and potential outcome.

A small number of studies (Table 1) have applied metabolomics to investigate COVID-19 in human patients, (Blasco et al., 2020; Kimhofer et al., 2020; Overmyer et al., 2020; Shen et al., 2020; Thomas et al., 2020). These have highlighted disruption of lipid metabolism (Overmyer et al., 2020; Thomas et al., 2020) along with tryptophan metabolism in relation to inflammation (Blasco et al., 2020; Overmyer et al., 2020; Thomas et al., 2020) and changes in pyrimidine metabolism (Blasco et al., 2020) as metabolic features of COVID-19 patients against controls. Some of these studies were clearly limited by patient numbers and may therefore not be fully representative of the variation in human responses to COVID-19, and some lacked proper statistical tests (see (Broadhurst and Kell, 2006)). Moreover, many of these markers of COVID-19 infection, severity and outcome have also been described in patients with sepsis and acute respiratory failure (Migaud et al., 2020). Most importantly, they tended simply to compare patients with healthy controls, which given that the disease status is in fact known does not of itself have either diagnostic or prognostic value. We here ask a more pertinent question in a well-powered study: can the metabolome distinguish patients with COVID-19 in terms of either disease severity (mild/severe) or outcome (deceased/survived)?

medRxiv preprint doi: https://doi.org/10.1101/2020.12.09.20246389; this version posted December 11, 2020. The copyright holder for this preprint **(which was not certified by peer review)** is the author/funder, who has granted medRxiv a license to display the preprint in perpetuity.

It is made available under a CC-BY-ND 4.0 International license .

Table 1. Overview of findings and study design in published studies utilising metabolomics to assess COVID-19 diagnosis, severity and outcome.

Reference	Sample types and numbers	Outcome	Metabolites/Metabolic pathways	Targeted/untargeted
(Blasco et al., 2020)	Plasma from time of COVID-19 diagnosis based on SARS-CoV-2 PCR for COVID-19 patients vs control patients (does not provide details). Patient numbers: 55 COVID-19 patients vs 45 controls	Predict: diagnosis from metabotype and COVID-19 disease evolution (Day 7 and Day 15)	Cytosine and tryptophan metabolism as marker of SARS-CoV-2 infection and COVID-19 severity/outcome	Targeted LC-MS based on MSML, IROA
(Shen et al., 2020)	Serum from patients with COVID-19 diagnosis vs patients with similar symptoms but negative SARS-CoV-2 RTPCR or healthy control subjects. Patient numbers: - 28 severe COVID-19 - 25 non-severe COVID-19 - 28 healthy subjects - 25 non-COVID-19 (COVID-19 symptoms, negative test)	Differences in proteomic and metabolomic profiles of COVID-19 vs healthy controls.	Dysregulated lipid, amino acid and kynurenine metabolism. Increased kynurenine pathway metabolite levels in COVID-19 patients Reduction in levels of many lipids in COVID-19 patients vs controls Reduced levels of amino acids and derivatives, particularly metabolites of arginine metabolism, in COVID-19 patients vs controls	Untargeted LC-MS/MS
(Overmyer et al., 2020)	Plasma on hospital admission with moderate to severe respiratory issues with suspected SARS-CoV-2 infection. Those with negative COVID-19 test outcome assigned to controls. Patient numbers: 102 COVID-19 vs 26 non-COVID-19 (COVID-19 symptoms, negative test)	Prediction of COVID-19 severity along with proteomic and transcriptomic data	Lipids and tryptophan metabolites associated with COVID-19 severity.	GC-MS and AEX-LC-MS/MS. Semi-targeted
(Thomas et al., 2020)	Serum samples. Day of sample draw not specified. Some controls were COVID-19 convalescent patients (negative for SARS-CoV-2 RTPCR) Sample numbers: 33 COVID-19 vs 16 controls	Observational study	Alterations in metabolism of lipids, amino acids (particularly tryptophan and arginine) in COVID-19 patients.	Untargeted and targeted LC-MS/MS
(Kimhofer et al., 2020)	Plasma from 17 adults with positive SARS-CoV-2 test result vs 25 healthy controls from general population	Differentiate SARS-CoV-2 infected patient from controls	Alterations in lipid and amino acid metabolism, particularly tryptophan metabolism in COVID-19 vs healthy patients.	NMR and targeted LC-MS of amino acids

Abbreviations: MSML IROA, Mass Spectrometry Metabolite Library supplied by IROA Technologies; GC-MS: Gas Chromatography-Mass Spectrometry; AEX-LC-MS/MS: Anion Exchange-Liquid Chromatography-Tandem Mass Spectrometry; NMR: Nuclear Magnetic Resonance.

To that end, we adopted an untargeted metabolomics approach using LC-MS/MS to cohorts of serum samples collected at the Royal Liverpool University Hospital (RLUH). 120 patient samples were obtained at the time of admission and diagnosis with COVID-19. This study enabled us to identify prognostic biomarkers of both COVID-19 severity (severe *vs* mild) and outcome.

medRxiv preprint doi: https://doi.org/10.1101/2020.12.09.20246389; this version posted December 11, 2020. The copyright holder for this preprint **(which was not certified by peer review)** is the author/funder, who has granted medRxiv a license to display the preprint in perpetuity.

It is made available under a CC-BY-ND 4.0 International license .

Here we present the study results via a set of different models. We first validate that untargeted metabolomics provides better severity and outcome distinction *vs* using solely demographics and clinical data, via multiblock analysis. A high dimensional predictive model is then presented, based on more than 900 metabolites, showing promising predictive performance. Next, with the goal of clinical application in mind, we present predictive model results of 20 compounds selected on the basis of our confidence in the metabolites' identity and known biological function. We discuss in detail the approaches used to make this selection via pathway enrichment analysis and manual curation. Finally, we explore (and largely discount) the possible confounding effects of demographic factors and underlying conditions of the selected metabolic predictors.

Results

LC-MS data preprocessing in Compound Discoverer resulted in 5234 ESI+ and 2465 ESI- retained metabolic features. The excluded features resulted from the standard filters; i.e., background compounds, features with quality control (QC) samples coefficient of variation (CV) >30 % or presence in less than 80 % of the QCs. Additionally, compounds detected in less than 25 % of the experimental samples were also excluded. The latter allowed the removal of a large number of metabolites related to drugs and their metabolites taken by the patients for preexisting conditions, which would otherwise simply have represented confounders.

Exploratory analysis

Principal components analysis (PCA) was performed on both positive electrospray ionization (ESI+) and negative electrospray ionization (ESI-) data and no clear clustering due to either severity or outcome could be observed (Figure S1), indicating that a simple, unsupervised method such as PCA had failed to detect differences in metabolic profiles related to COVID-19 infection and potential outcome in complex data resulting from LC-MS analysis. In contrast, when PCA was applied to the metadata associated with the 120 patients which include gender, age, body mass index (BMI), pulse, temperature, blood pressure, respiratory rate (full list is provided in the methods section), a trend of separation between severe and mild patients was observed (Figure 1A). This alone is not overly interesting because the severity assessment was drawn from a few variables in these metadata. However, when the metadata and the LC-MS ESI+/- data were analyzed together by using a multiblock PCA (Smilde et al., 2005; Xu and Goodacre, 2012) the separation trend improved (Figure 1B). Those observations are also valid in fatal outcomes where no clear clustering is observed in the metadata PCA block (Figure 1A). Individual block figures from the multiblock analysis are available in the supplementary information (Figure S2). Clearly PCA is not a classification technique and the lack or presence of clusters does not translate directly to any predictive potential of the data. To explore if differences in metabolic profiles are capable of predicting the severity and outcome of COVID-19 infection, the next section explores in detail predictive models based on the LC-MS data.

Predictive models

Four multi-predictor models were trained: extreme gradient boosted tree (Chen and Guestrin, 2016; Friedman, 2001), Lasso regularization with elastic net (Zou and Hastie, 2005), logistic regression, and Bayesian logistic regression (Goodrich, 2020). All these models, when trained on the complete data of >7000 metabolic features, showed clear signs of overfitting despite the use of cross-validation and regularization. To overcome this, the set of predictors were filtered based on individual significance as determined by volcano plot analysis (p-value and fold change) as illustrated in Figure 2 for outcome. Volcano plots for severity are available in the Supplementary information (Figure S3).

medRxiv preprint doi: https://doi.org/10.1101/2020.12.09.20246389; this version posted December 11, 2020. The copyright holder for this preprint **(which was not certified by peer review)** is the author/funder, who has granted medRxiv a license to display the preprint in perpetuity.

It is made available under a CC-BY-ND 4.0 International license .

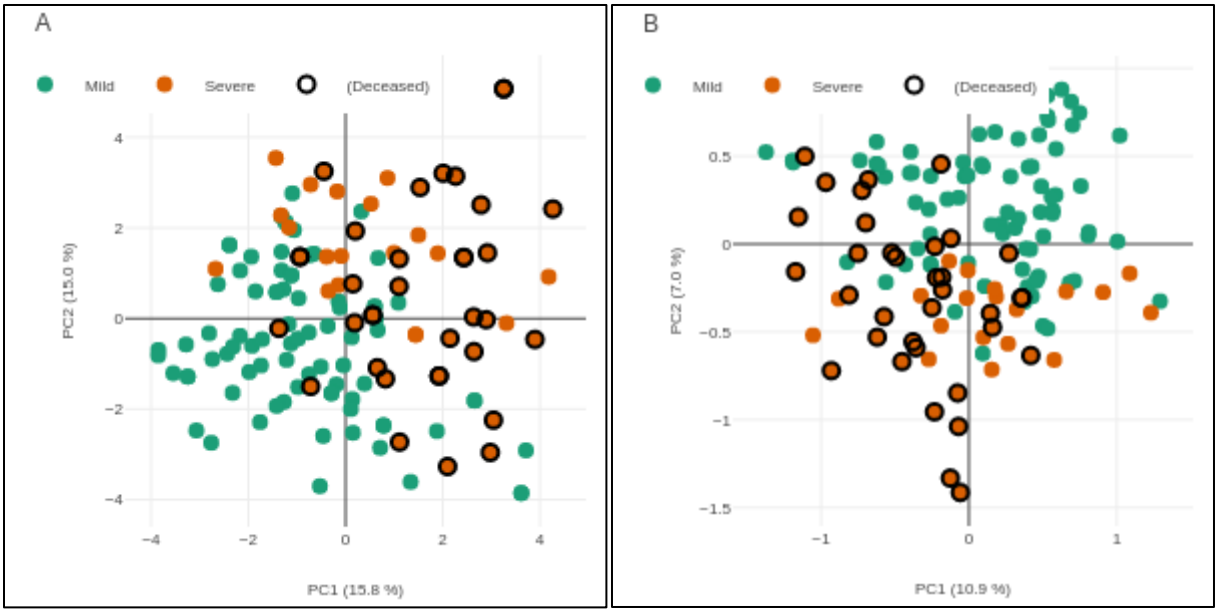

Figure 1. Metadata alone (A) and multiblock (B) PCA for severity and outcome. It can be observed that group separation trends improve with addition of LC-MS data (B). It is important to note that deceased patients are a subset of severe cases that do not appear to show specific clustering in this exploratory analysis. Axis are labelled with principal component and its explained variance in percentage.

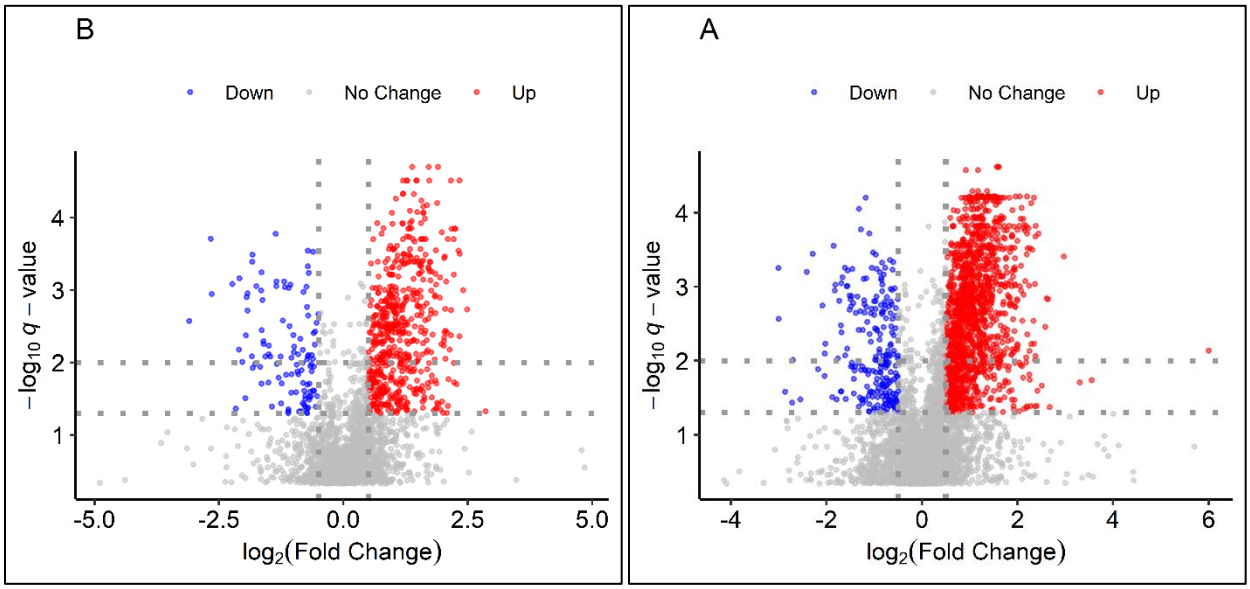

Figure 2. Volcano plots ESI+(A) and ESI-(B) for metabolites discriminating disease outcome. Dotted lines mark boundary of significance 0.5 for Log_2 Fold Change (FC) 0.05 for *q*-value at 0.05 with second dotted for *q*-value at 0.01. Compounds with higher levels in poor outcome are coloured in red and inversely compounds with significantly lower levels in blue. It can be observed that in both ESI+ and ESI- differences in fatal outcome are more often based on increased levels.

Significance filtering based on volcano analysis reduced the number of metabolic features to 1987/ 937 (ESI+/- respectively) for severity and/or outcome combined. For those features, signal curation based on chromatogram and spectral quality (see Methods section), was performed in Compound Discoverer and a total of (526/409 ESI+/- respectively) features were retained. Table 2 below provides a breakdown of those

medRxiv preprint doi: https://doi.org/10.1101/2020.12.09.20246389; this version posted December 11, 2020. The copyright holder for this preprint (which was not certified by peer review) is the author/funder, who has granted medRxiv a license to display the preprint in perpetuity.

It is made available under a CC-BY-ND 4.0 International license .

compounds in terms of Metabolomics Standards Initiative (MSI) levels (Sumner et al., 2007), ranging from MSI level 1 to 4.

Table 2. Number of metabolic features remaining after LC-MS/MS data pre-processing, statistical selection of significant features and manual curation for chromatographic peak shape and spectral signal. Compounds where no molecular formula could be assigned by CD3.1 (see Methods) were discarded.

MSI level (Sumner et al., 2007)	ESI+	ESI-
Level 4: Molecular formula match	526	409
Level 3: Molecular formula + Mass library match	384	283
Level 2: all above plus MS/MS match (spectral match ≥ 70 %)	45	33
Level 1: MS/MS experimental in-house library match	14	8

Evaluation of the four predictive models on this reduced set of 937 ESI+/- metabolic features showed best generalization results using Bayesian logistics regression; therefore, all the following results are based on this model. The mean area under the curve (AUC) was calculated at 0.836 (SD 0.069) for severity and 0.807 (SD 0.081) for outcome, demonstrating good predictive power of the patient metabolome. However, a mass spectrometry-derived model with some 900 compounds is not a practical solution (Kenny et al., 2010) for an assay of general utility, and thus subsets of these compounds were investigated further. The sub-group selection was guided by metabolic pathway enrichment analysis and manual curation of well identified (i.e. MSI level 1 or 2) compounds with known biological activity. A final model with 20 compounds selected in this way showed a reasonable cross-validated mean AUC of 0.793 (SD 0.080) for severity and 0.792 (0.090) for outcome. Mean balanced accuracy was calculated at 0.716 (0.088) and 0.655 (0.098) for severity and outcome, respectively. Representative receiver operating characteristic (ROC) curves for one random train-test split are shown in Figure 3.

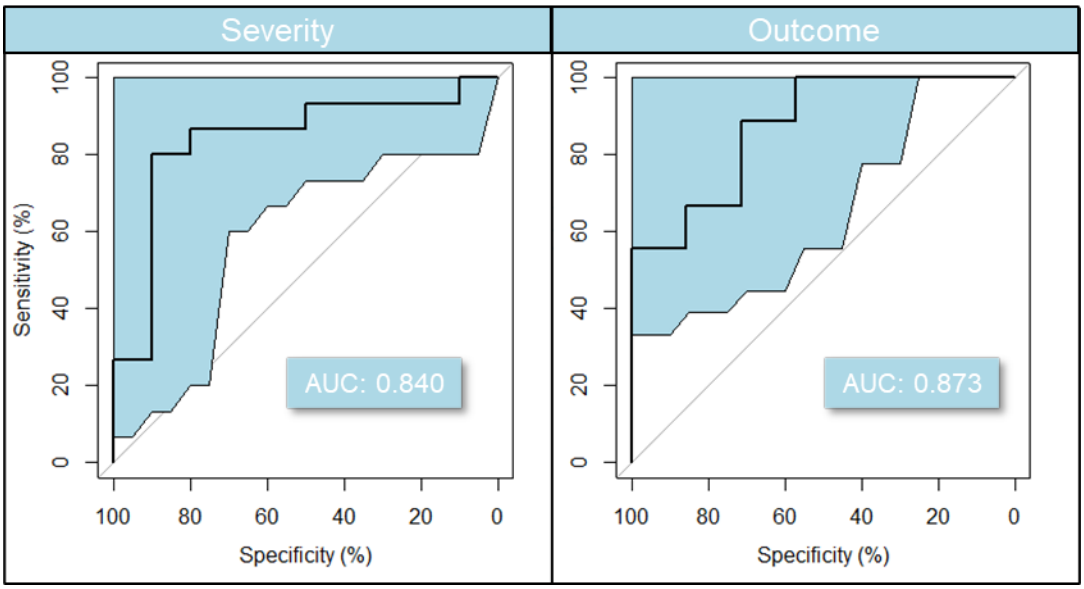

Figure 3. Predictive model based on 20 compounds selected for their identification confidence and known biological role (see Figure 4). Balanced accuracy and AUC for the represented in the graphic model are in the 0.70s and 0.80s, respectively. ROC 95% confidence intervals were calculated with 2000 stratified bootstrap replicates on the test data and are presented as blue shading around the mean curve. A Monte Carlo cross-validation results estimate the model balanced accuracy at 0.716 for severity and 0.655 for outcome. Cross-validated AUC was calculated at ~0.79 in both conditions.

medRxiv preprint doi: https://doi.org/10.1101/2020.12.09.20246389; this version posted December 11, 2020. The copyright holder for this preprint **(which was not certified by peer review)** is the author/funder, who has granted medRxiv a license to display the preprint in perpetuity.

It is made available under a CC-BY-ND 4.0 International license .

Metabolic pathways linked to severity and outcome

Pathway enrichment analysis was performed with MUMMICHOG (Li et al., 2013) as implemented in MetaboAnalyst (Pang et al., 2020) as a way of selecting biologically relevant sub-groups of compounds. As expected, no 'entire' pathways showed significant *p*-values when ESI+ and ESI- results were grouped together (Anderson et al., 2014; Kell and Goodacre, 2014; Kell and Westerhoff, 1986). However, pathways that showed multiple significant hits were further investigated manually. These included pyrimidine metabolisms, tryptophan metabolism, and aspartate and asparagine metabolism. A number of these are in accordance with recently published studies comparing COVID-19 patients to healthy controls (Blasco et al., 2020; Overmyer et al., 2020; Thomas et al., 2020). The 20 compounds selected with this approach (shown with their significance in patient outcome Figure 4) are further discussed below. Selected compound significance in the prediction of COVID-19 severity is shown in Figure S4.

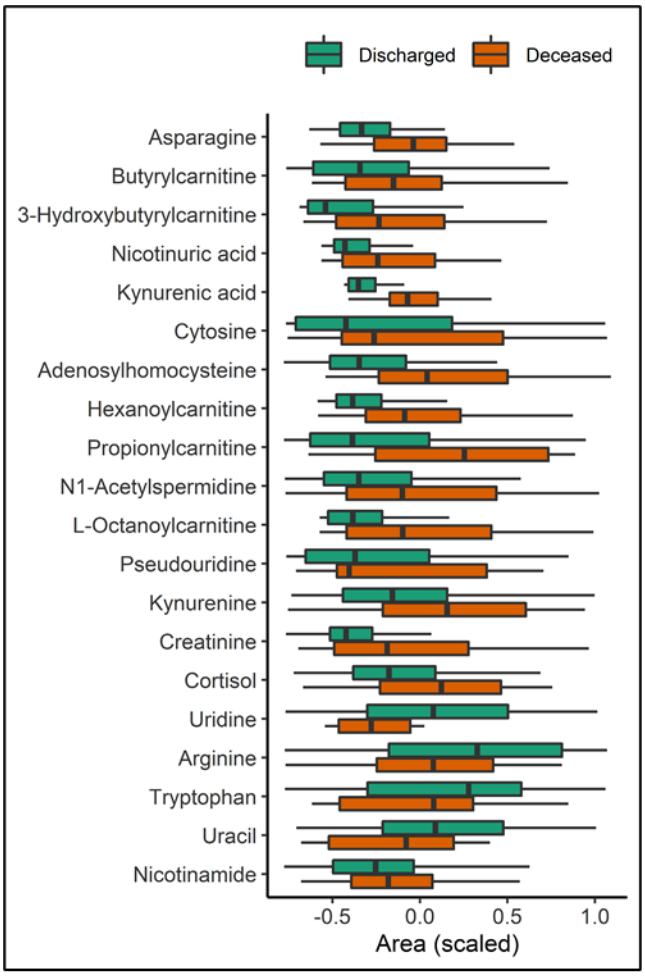

Compounds retained for severity and outcome predictive model and their significance in fatal outcome

Name	Polarity	MSI	FC	*q*-value
Asparagine	ESI+	3	2.42	**
Butyrylcarnitine	ESI+	1	2.37	**
3-hydroxybutyrylcarnitine	ESI+	3	2.35	***
Nicotinuric acid	ESI+	3	2.33	***
Kynurenic acid	ESI-	1	2.29	***
Cytosine	ESI+	1	2.21	***
Adenosylhomocysteine	ESI+	1	2.03	***
Hexanoylcarnitine	ESI+	2	1.77	***
Propionylcarnitine	ESI+	1	1.77	***
N1-acetylspermidine	ESI+	3	1.74	**
L-Octanoylcarnitine	ESI+	1	1.72	**
Pseudouridine	ESI-	1	1.71	**
Kynurenine	ESI+	1	1.58	***
Creatinine	ESI+	2	1.54	**
Cortisol	ESI+	1	1.36	**
Uridine	ESI-	1	0.76	**
Arginine	ESI+	1	0.79	**
Tryptophan	ESI+	1	0.88	
Uracil	ESI+	1	0.91	
Nicotinamide	ESI+	1	1.06	

Figure 4. Compounds retained for severity and outcome predictive model. Box plot shows compound area differences between discharged and deceased patients ordered by fold change. Compounds areas are standardized (mean = 0, SD = 1) to facilitate comparison. Boxes represent the interquartile rage Q1 to Q3 with Q2 (i.e. median) line in the middle. Outliers range is depicted by the 'whiskers'. The table on the right side of the figure shows detailed information about the compounds including FC and *q*-value (false discovery rate corrected *p*-value) following 'star' notation i.e. '***' correspond to *q*-values <0.001, '**' <0.01, and missing when >0.1.

Elevated serum cytosine association with severity and outcome

Cytosine levels were increased over 2-fold in patient samples at admission who went on to develop severe symptoms or subsequently died (Figure 5 A and B). Furthermore, cytosine:uracil ratios showed a comparable separation. Elevated cytosine levels were also found in COVID-19 patients measured against

medRxiv preprint doi: https://doi.org/10.1101/2020.12.09.20246389; this version posted December 11, 2020. The copyright holder for this preprint **(which was not certified by peer review)** is the author/funder, who has granted medRxiv a license to display the preprint in perpetuity.

It is made available under a CC-BY-ND 4.0 International license .

healthy controls and 15 days post infection in (Blasco et al., 2020), but severity or outcome were not discriminated as they were here.

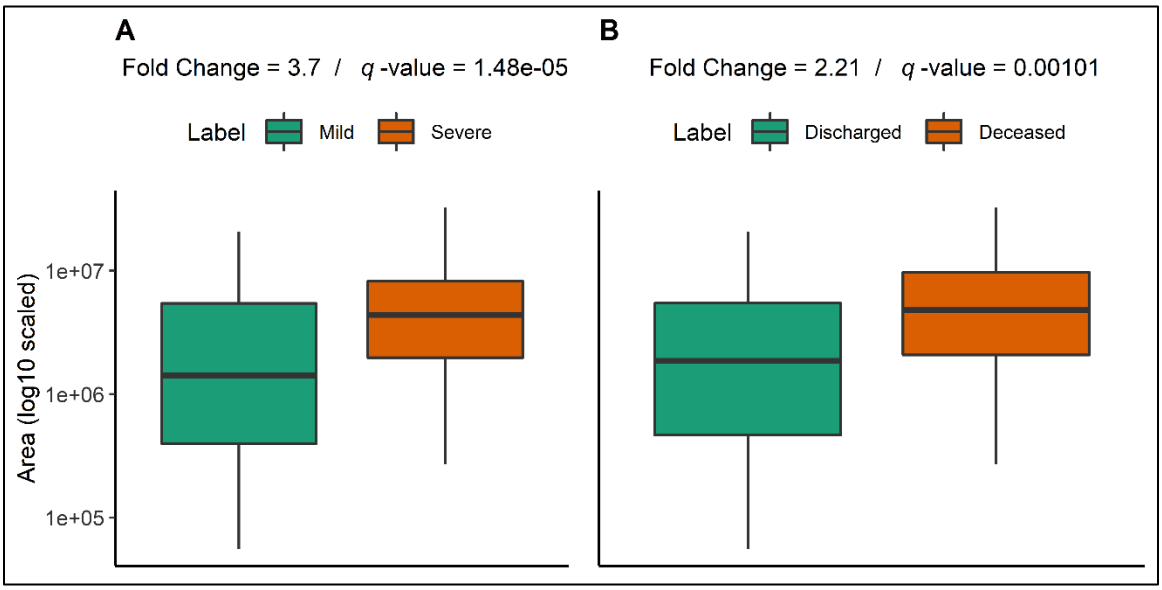

Figure 5. Cytosine levels in patients according to (A) severity or (B) outcome. Boxplot markings follow the same standard as Figure 4.

Uridine, another pyrimidine, was found significantly decreased in fatal outcome cases; however, its Log Fold Change (LFC) was close, but not significant in severe cases. Moreover, pseudouridine, an isomer of uridine, was increased in patient samples with severe disease progression or deceased outcome. Pseudouridine (Figure 4) is a marker of cell ribosomal RNA (rRNA) turnover (Nakano et al., 1993), for instance in heart failure (Dunn et al., 2007).

Tryptophan and kynurenine metabolism compounds associate with both severity and outcome

Kynurenine (a tryptophan degradation product, see schematic in Figure 6) was significantly increased in both severe cases and in patients who died, with a fold change of 1.5. The difference was even more marked for kynurenic acid in outcome, with levels increasing over 2-fold.

In addition to changes in kynurenine and kynurenic acid, our results showed that a reduction in levels of serotonin (MSI level 3) and melatonin (MSI level 3) were associated with severity and death. We also observed an increase in serum levels of cortisol with *q*-value of 0.006 and ~1.3-fold in severe cases as well as those who died. The observed changes in tryptophan metabolism appear to be related to an immune response to SARS-CoV-2 since tryptophan dioxygenase, a tryptophan-degrading enzyme, activity is upregulated by cortisol and initiates degradation of tryptophan to kynurenine. Previous research (Thomas et al., 2020) has found a correlation between increases of interleukin 6 and kynurenine levels in COVID-19 patients compared to controls. Finally, kynurenine pathway upregulation as part of an inflammatory response is known to impact serotonin levels negatively (Hunt et al., 2020; Li et al., 2017), as also observed in our results.

medRxiv preprint doi: https://doi.org/10.1101/2020.12.09.20246389; this version posted December 11, 2020. The copyright holder for this preprint **(which was not certified by peer review)** is the author/funder, who has granted medRxiv a license to display the preprint in perpetuity.

It is made available under a CC-BY-ND 4.0 International license .

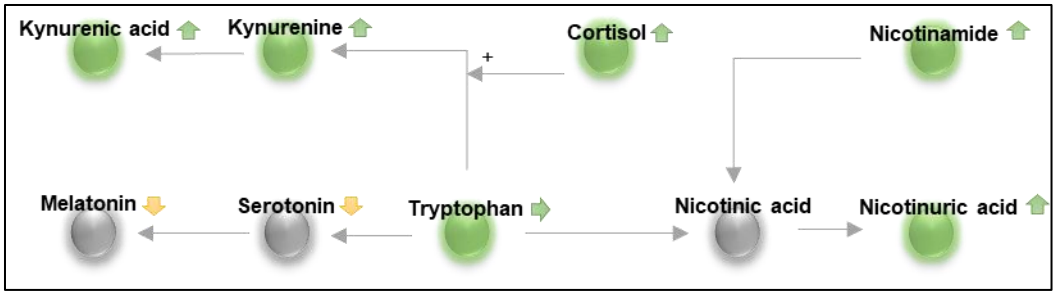

Figure 6. Simplified schematic representation of tryptophan metabolism highlighting connections to compounds discussed in this section. Compounds marked with green background are part of our predictive model. Arrows indicated the change in severity or outcome and arrows green colour indicate good confidence in compound identification (i.e. MSI level 1 or 2).

Interestingly we observed nicotinamide (MSI 1) levels to be 1.5-fold higher in severe case, but not significant in outcome. Conversely, nicotinuric acid (MSI 3) levels were over 2-fold higher in fatal outcome and non-significant in severity. Both nicotinamide and nicotinuric acid are related to kynurenine/tryptophan metabolism (Murray, 2003), and forms of nicotinic acid (i.e. niacin or vitamin B3). It is important to note that niacin was not detected in the experiment and was not reported as part of any patient's treatment.

Beta oxidation metabolites, acylcarnitines, increased in severe and deceased outcome patients

Multiple fatty acyl carnitines, e.g. hydroxybutyrylcarnitine (>2-fold), hexenoylcarnitine (1.4-fold) and hydroxyoctanoyl (~2 fold), were found to be significantly higher in both severe and poor outcome cases. Long chain fatty acyl carnitines were not reliably detected in the study as the LC gradient used for data acquisition is optimized for more hydrophilic molecules. Therefore, fatty acyl carnitines with more than 10-carbon FA chains were excluded from the analysis. On the other hand, carnitine (MSI level 1) and its precursors, i.e. lysine (MSI 1) and methionine (MSI 1), were unchanged in severity and outcome.

Other compounds

The final selection of compounds also includes the amino acids arginine (MSI level 1) and asparagine (MSI level 3); asparagine showed more than a 2-fold change in poor outcome and 1.7-fold in severe cases. Additionally, *S*-adenosylhomocysteine (MSI level 2), a precursor to homocysteine showed significantly increased levels in severe cases and fatal outcome conditions. Moreover, the model includes *N*-acetylspermidine (MSI level 3) that was reported along with spermidine by (Thomas et al., 2020) as increased in COVID-19 patient sera compared to controls. Interestingly, in contrast to *N*-acetylspermidine, spermidine did not show significant changes in relation to either severity or outcome. Finally, the model includes creatinine (MSI level 2) which, in accordance with the clinically acquired data, tend to increase in patients with fatal outcomes but did not increase with disease severity.

Model compounds adjusted for demographic factors and underlying conditions

Confounders are an important issue in omics studies (Broadhurst and Kell, 2006), and several factors (age, gender, BMI, and existing inflammatory diseases) are recognised as predisposing patients infected with COVID-19 to severe infection and poor outcome. Any impact on compound levels simply from population demographics and underlying conditions was explored with univariate logistic regression odds ratios (OR) and 95% confidence interval (95% CI) analysis. Individual compounds' odds ratio (OR) and 95% confidence intervals (CI) for outcome as adjusted for age, gender, BMI, diabetes, liver, kidney and cardiac disease and all together are presented in Table 3. The severity-based table is available in the supplementary information (Table S1). It is important to note that identifying links between those factors and the compounds of interest is meaningful when evaluating their biological role; however, being 'confounded' does not invalidate their predictive power and relevance in a predictive model. Additionally, it can be observed that not all compounds (e.g. kynurenic acid, cortisol) selected for their significant *q*-value and fold change showed significance based on 95% CI.

medRxiv preprint doi: https://doi.org/10.1101/2020.12.09.20246389; this version posted December 11, 2020. The copyright holder for this preprint **(which was not certified by peer review)** is the author/funder, who has granted medRxiv a license to display the preprint in perpetuity.

It is made available under a CC-BY-ND 4.0 International license .

An important result from this analysis is that cytosine and kynurenine remained significant regardless of patient demographics or underlying conditions. By contrast, increases in levels of short and medium fatty acylcarnitines in severity and outcome appear to be partially explained by age and BMI, as their OR tended to decrease when adjusted, and this may be correlated to frailty in ageing (Rattray et al., 2019). After adjusting for all recorded conditions in the study, only butyrylcarnitine, 3-hydroxybutyrylcarnitine and hydroxyhexanoycarnitine showed a strong relation to disease severity. In respect to outcome, butyrylcarnitine remained the most significant. This indicates that higher levels of acyl carnitines are likely linked to metabolic differences in the patients prior to the viral infection. As such they could potentially indicate a risk group. Moreover, pseudouridine's significance was impacted by age, BMI and mildly by cardiac conditions and hypertension. This in itself is not a confounding issue since both age and BMI also contribute statistically to the outcome of COVID-19 (Hussain et al., 2020; Iaccarino et al., 2020).

Interestingly asparagine, despite maintaining strong significance while adjusted for all factors showed an increased OR when adjusted for age in fatal outcome case. In contrast asparagine OR dropped when adjusted for age and BMI in severe (vs mild) cases. Lower asparagine levels have also been associated with an increased risk of developing type 2 diabetes mellitus and coronary artery disease (Ottosson et al., 2018).

Discussion

In this study we employed untargeted metabolomics using LC-MS/MS to detect and measure changes in the baseline serum metabolome of a cohort of 120 COVID-19-infected patients at the point of hospital admission. Our aim was to find not only prognostic markers of subsequent disease severity and outcome, but to also understand what effects COVID-19 infection has on the patient's metabolome and inversely what effect patient biochemistry and physiology have on infection development. These results could then be used to guide patient treatment and medical attention requirements following COVID-19 diagnosis. Most studies to date applying metabolomics to COVID-19 human patients have compared them against healthy controls; this is of limited predictive value, as rapid PCR and antibody tests exist, and does not provide an insight into what biochemical changes drive disease severity or outcome. Moreover, a number of these studies (Table 1), used a small number of patients with limited variation in human responses to COVID-19, and some lacked proper statistical analysis (see (Broadhurst and Kell, 2006; Trivedi et al., 2017)).

Our results showed that distinct alterations in the serum metabolome were already capable of distinguishing both subsequent COVID-19 severity and outcome (discharge *versus* deceased) at the time of diagnosis and admission. More importantly, using both univariate and a multiple predictor Bayesian logistic regression model we found a subset of 20 metabolites with relevant biological functions that are predictive of subsequent disease severity and patient outcome with AUC 0.792 and 0.793 respectively. These changes centered particularly around pyrimidine, tryptophan and acylcarnitine metabolism, which can be related to viral replication, host inflammation response and alterations in energy metabolism.

Table 3. Adjusted logistic regression results by outcome. Positive OR indicate increased levels in patients with poor outcome and are presented with OR (95% CI). Significance is presented in 'star' notation i.e. '***' correspond to *p*-values <0.001, '**' <0.01, '*' <0.05, '.' < 0.1 and missing when >0.1. Compounds are adjusted for age, gender, BMI, liver conditions, cardiovascular diseases, hypertension, kidney disease, diabetes and all together. Details of specific diseases in each category are available in the Methods section.

	Adjusted by:	None		Age		Gender		BMI		Liver disease		CV disease		Hypertension		Kidney disease		Diabetes		All	
	Compound	OR	Sig.	OR	Sig.	OR	Sig.	OR	Sig.	OR	Sig.	OR	Sig.	OR	Sig.	OR	Sig.	OR	Sig.	OR	Sig.
Nucleic acids metabolism	Cytosine	2.1 (1.4-3.6)	**	2 (1.2-3.4)	*	2.3 (1.4-3.9)	**	2.1 (1.3-3.8)	**	2.1 (1.4-3.6)	**	2.1 (1.3-3.5)	**	2 (1.3-3.4)	**	2 (1.3-3.5)	**	2 (1.3-3.5)	**	2.5 (1.4-4.9)	**
	Uracil	0.75 (0.47-1.1)		0.84 (0.56-1.2)		0.79 (0.49-1.2)		0.83 (0.56-1.2)		0.75 (0.47-1.2)		0.72 (0.44-1.1)		0.78 (0.48-1.2)		0.79 (0.49-1.2)		0.79 (0.49-1.2)		0.81 (0.45-1.4)	
	Pseudouridine	1.9 (1.3-2.8)	**	1.5 (0.97-2.4)	.	1.9 (1.2-2.9)	**	1.6 (1.1-2.5)	*	1.9 (1.3-2.8)	**	1.8 (1.2-2.8)	**	1.7 (1.1-2.7)	*	2 (1.2-3.5)	*	2 (1.2-3.5)	*	1.6 (0.91-2.9)	
	Uridine	0.39 (0.21-0.67)	**	0.58 (0.37-0.88)	*	0.4 (0.22-0.7)	**	0.61 (0.39-0.91)	*	0.39 (0.21-0.67)	**	0.36 (0.19-0.63)	***	0.41 (0.22-0.7)	**	0.41 (0.22-0.71)	**	0.41 (0.22-0.71)	**	0.41 (0.19-0.82)	*
Kynurenine metabolism	Tryptophan	0.71 (0.46-1.1)		0.88 (0.59-1.3)		0.68 (0.43-1.1)	.	0.79 (0.53-1.2)		0.72 (0.46-1.1)		0.72 (0.46-1.1)		0.73 (0.47-1.1)		0.76 (0.48-1.2)		0.76 (0.48-1.2)		0.72 (0.42-1.2)	
	Kynurenine	2.7 (1.7-4.8)	***	2.3 (1.4-4.2)	**	2.8 (1.8-5.1)	***	2.3 (1.4-3.9)	**	2.7 (1.7-4.8)	***	2.9 (1.7-5.4)	***	2.6 (1.6-4.6)	***	2.6 (1.6-4.7)	***	2.6 (1.6-4.7)	***	2.6 (1.5-5)	**
	Kynurenic acid	1.5 (0.99-2.6)		1.4 (0.91-2.7)		1.5 (0.96-2.6)		1.4 (0.88-2.6)		1.5 (0.98-2.6)		1.5 (1-2.6)	.	1.4 (0.91-2.4)		1.3 (0.87-2.4)		1.3 (0.87-2.4)		1.2 (0.73-2.1)	
	Cortisol	1.4 (0.93-2.2)		1.3 (0.9-2.1)		1.4 (0.93-2.2)		1.2 (0.82-2)		1.4 (0.94-2.2)		1.4 (0.91-2.1)		1.4 (0.92-2.2)		1.4 (0.93-2.1)		1.4 (0.93-2.1)		1.4 (0.86-2.3)	
	Nicotinamide	1.1 (0.68-1.5)		1.2 (0.8-1.8)		1 (0.67-1.5)		1 (0.69-1.5)		1 (0.67-1.5)		1.1 (0.68-1.5)		1.1 (0.69-1.6)		1.1 (0.67-1.5)		1.1 (0.67-1.5)		1.2 (0.7-1.9)	
	Nicotinuric acid	1.6 (1.1-2.6)	*	1.5 (1-2.8)	.	1.6 (1.1-2.5)	*	1.6 (1-2.9)	.	1.7 (1.1-2.7)	*	1.6 (1.1-2.6)	*	1.5 (1-2.4)	*	1.5 (1-2.6)	.	1.5 (1-2.6)	.	1.5 (0.92-2.6)	
Fatty acyl carnitines	Propionylcarnitine	2.2 (1.5-3.6)	***	2 (1.3-3.2)	**	2.2 (1.4-3.5)	***	1.9 (1.2-3)	**	2.3 (1.5-3.6)	***	2.2 (1.4-3.5)	***	2.1 (1.4-3.5)	***	2.2 (1.4-3.5)	**	2.2 (1.4-3.5)	**	1.9 (1.1-3.2)	*
	Butyrylcarnitine	2.5 (1.6-4.4)	***	2.8 (1.6-5.7)	**	2.5 (1.6-4.5)	***	2.3 (1.3-4.4)	**	2.6 (1.6-4.6)	***	2.5 (1.5-4.4)	***	2.4 (1.5-4.3)	***	2.4 (1.5-4.3)	***	2.4 (1.5-4.3)	***	2.2 (1.3-4.4)	*
	3-hydroxybutyrylcarnitine	1.9 (1.3-2.9)	**	1.7 (1.1-2.8)	*	2.1 (1.4-3.3)	***	1.5 (0.98-2.4)	.	1.9 (1.3-2.9)	**	1.8 (1.2-2.9)	**	1.8 (1.2-2.9)	**	1.8 (1.2-2.8)	**	1.8 (1.2-2.8)	**	1.6 (1-2.7)	*
	Hexanoylcarnitine	1.4 (0.95-2.4)		1.2 (0.82-2.2)		1.4 (0.92-2.3)		1.3 (0.83-2.2)		1.4 (0.95-2.4)		1.4 (0.93-2.3)		1.3 (0.9-2.3)		1.3 (0.88-2.2)		1.3 (0.88-2.2)		1.1 (0.67-1.7)	
	L-Octanoylcarnitine	1.4 (0.93-2.2)		1.2 (0.78-1.9)		1.3 (0.9-2.2)		1.2 (0.79-1.9)		1.4 (0.93-2.2)		1.3 (0.91-2.2)		1.3 (0.87-2.1)		1.3 (0.84-2.1)		1.3 (0.84-2.1)		0.95 (0.56-1.5)	
Other	Creatinine	1.5 (1-2.4)	*	1.4 (0.91-2.2)		1.5 (1-2.3)	.	1.4 (0.93-2.4)		1.5 (1-2.4)	*	1.6 (1.1-2.4)	*	1.4 (0.93-2.2)		1.4 (0.91-2.3)		1.4 (0.91-2.3)		1.4 (0.82-2.4)	
	Asparagine	2.8 (1.4-6.9)	*	7.5 (2.8-24)	***	2.7 (1.4-6.5)	*	3.2 (1.4-8.4)	**	2.8 (1.4-6.9)	*	3 (1.5-7.3)	**	3.9 (1.8-10)	**	3.2 (1.5-8.3)	**	3.2 (1.5-8.3)	**	4.5 (1.8-14)	**
	Arginine	0.53 (0.33-0.81)	**	0.66 (0.43-0.97)	*	0.52 (0.32-0.81)	**	0.69 (0.46-1)	.	0.51 (0.32-0.8)	**	0.53 (0.33-0.81)	**	0.53 (0.33-0.82)	**	0.55 (0.34-0.86)	*	0.55 (0.34-0.86)	*	0.59 (0.33-1)	.
	N1-acetylspermidine	1.9 (1.3-3)	**	1.8 (1.2-3.1)	*	1.9 (1.3-3.1)	**	1.7 (1.1-2.9)	*	2 (1.3-3.2)	**	1.9 (1.2-3)	**	1.9 (1.3-3.1)	**	1.8 (1.2-2.9)	**	1.8 (1.2-2.9)	**	1.7 (1-3)	*
	Adenosylhomocysteine	2.3 (1.4-4.2)	**	2.2 (1.3-4.5)	*	2.3 (1.4-4.4)	**	2.3 (1.3-4.7)	*	2.3 (1.4-4.2)	**	2.2 (1.4-4.1)	**	2.2 (1.3-4.1)	**	2.3 (1.3-4.8)	*	2.3 (1.3-4.8)	*	2.1 (1.2-4.3)	*

medRxiv preprint doi: https://doi.org/10.1101/2020.12.09.20246389; this version posted December 11, 2020. The copyright holder for this preprint (which was not certified by peer review) is the author/funder, who has granted medRxiv a license to display the preprint in perpetuity.

It is made available under a CC-BY-ND 4.0 International license .

Alterations in pyrimidine metabolites predictive of severity and outcome

Viral infections induce characteristic changes in host cell metabolism to enable effective viral replication (Thaker et al., 2019). Moreover, the resulting metabolic impact and cellular reprogramming varies between viruses (even within the same family) and host cell type. In the case of SARS-CoV-2, cytosine has been described as pivotal in the virus' evolution (Danchin and Marlière, 2020) where avoidance of host defense mechanisms have favored a reduced cytosine proportion in viral RNA, estimated at 17.6 %. When compared to typical human RNA, the cytosine proportion is significantly lower. In contrast to cytosine, the proportion of uracil in SARS-CoV-2 is estimated at around 32.4 % (Danchin and Marlière, 2020) and it is significantly higher than that in human RNA. Consequently, the ratio of serum uracil to cytosine may be even more informative of the viral load and current reproduction activity in a patient. This difference between host and viral RNA composition could result in significant levels of cytosine being released into the circulation upon the death of infected cells. Therefore, higher levels of cytosine in blood can reasonably be expected to indicate higher levels of viral load.

Cytosine has been reported previosuly to discriminate between COVID-19 infection compared to uninfected individuals (Blasco et al., 2020) but has not been assessed regarding severity or outcome. Here, our analyses showed that cytosine levels were predictive of subsequent disease severity and outcome; serum cytosine levels were increased over 2-fold in serum from patient samples at admission who went on to develop severe symptoms or subsequently died (Figure 5 A and B). Given the reduced incorpration of cytosine into SARS-CoV-2, these results may indicate a higher viral load and replication, subsequently leading to the development of severe symptoms, in some cases resulting in death.

Increased viral reproduction activity could be due to an initial higher viral load, a host environment favorable to viral reproduction, or the effective stage of the infection. It is thus not possible to draw mechanistic conclusions from our results; nevertheless the cytosine OR remained stable when adjusted for demographic factors and known underlying conditions indicting that those factors are not significant with regard to viral replication rates. This would be more consistent with the fact that the initial load before admission is the most important parameter affecting both disease severity and outcome.

The serum cytosine:uracil ratio showed comparable resutls, with significant increase in severe cases and poor outcome. This result furthermore confirms the proposed relationship between pirimidines levels and viral activity based on (Danchin and Marlière, 2020) SARS-CoV-2 genome description.

Given these results, measurement of cytosine, uracil, and their ratios, could potentially allow tracking of viral activity and predict recovery or aggravation. However, it is important to note a limitation of cytosine:uracil ratio usage given that cytosine degradation pathway goes through uracil. To acknowledge this relationship, the kinetics of the degradation process need to be incorporated in a potential viral activity predictive model. Moreover, as highlighted by (Migaud et al., 2020) the levels of certain nucleobases are also increased in patients who die from sepsis and acute respiratory failure. Further investigation would be required to tease out the contributions of SARS-CoV-2 viral replication to the levels of these pyrimidines against the secondary effects of the virus on the host (human) health.

Pseudouridine, was also noted to be increased in severe cases and poor outcome. As mentioned previously pseudouridine (Figure 4) is a marker of cell (rRNA) turnover (Nakano et al., 1993), for instance in heart failure (Dunn et al., 2007). When adjusting for cardiovascular disease this compound remained significant but showed slight correlation with hypertension and age. Finally, when adjusted for all factors pseudouridine 95 % CI lost significance indicating correlation with more than one factor. Interestingly, growing evidence points toward complications in COVID-19 arising through a vasculopathy and coagulopathy elicited by the infection (Pretorius et al., 2020) and may be indicative of this process.

Tryptophan - kynurenine degradation

The degradation of tryptophan to kynurenine is a well-studied pathway associated with increased inflammatory processes. In the context of this study the non-significant decrease of tryptophan in severe

medRxiv preprint doi: https://doi.org/10.1101/2020.12.09.20246389; this version posted December 11, 2020. The copyright holder for this preprint **(which was not certified by peer review)** is the author/funder, who has granted medRxiv a license to display the preprint in perpetuity.

It is made available under a CC-BY-ND 4.0 International license .

cases could be explained either by change in dietary habits or more likely by the higher stimulation of tryptophan to kynurenine degradation indicated by the significant increase in levels of kynurenine and kynurenic acid. Upregulation of this process was further confirmed by the higher levels of cortisol, which stimulates tryptophan degradation, especially in severe cases (Table 3). An increase in patient kynurenine levels has also been reported in COVID-19 compared to controls in (Thomas et al., 2020), associated with severity in (Overmyer et al., 2020), and also linked to fatal sepsis development in (Migaud et al., 2020). This provides strong evidence of higher levels of immune response in severe cases and those with a fatal outcome. More recently, upregulation of tryptophan metabolites including kynurenine has been found to play a protective role in radiation injury during cancer radiotherapy (Guo et al., 2020) indicating that these relationships are more complicated than previously thought, and also involve the gut microbiome.

Furthermore, changes in levels of nicotinic acid reflected by its condensation product nicotinuric acid could possibly reflect a dysfunctional energy metabolism. Interestingly our data indicates increased levels of nicotinamide in severity and nicotinuric acid in outcome. Increased levels of nicotinuric acid in urine have been previously reported as pathogenic markers in metabolic syndrome and cardiovascular disease (Huang et al., 2013), again consistent with the known cardiovascular effects of SARS-CoV-2 infection (Fox et al., 2020; Grobler et al., 2020; Leisman et al., 2020; Libby and Lüscher, 2020; Paranjpe et al., 2020; Pretorius et al., 2020; Zheng et al., 2020).

Beta oxidation

Interestingly, levels of short and medium chain acylcarnitines were previously reported by (Thomas et al., 2020) as reduced in COVID-19 patients *versus* controls irrespective of Interleukin 6 (IL6) levels. In this study we identified multiple short chain acyl carnitines as increased in severe cases and those with a fatal outcome compared to mild cases and discharged patients. Changes in serum acylcarnitines have been previously associated with cardiovascular disease, diabetes and inflammation (Anderson et al., 2014). Moreover, increased levels of octanoyl-l-carnitine have been previously associate with arterial stiffness (Kim et al., 2015) and dysregulation of the carnitine shuttle. Long chain acyl carnitines, not detected in this study, have been additionally reported in relation to frailty (Rattray et al., 2019).

Indeed, adjusted logistic regression results (Table 3) here show that some of their significance can be explained by BMI levels. This could possibly indicate different levels change in energy metabolism as response to viral infection linked to preexisting phenotype i.e. BMI and therefore represent a high-risk group.

Compounds requiring further investigation

Our study highlighted a number of other compounds (not discussed here) that changed significantly in severity and outcome. However, as is common in metabolomics (Blaženović et al., 2018; Salek et al., 2013), these require further rigorous identification following Metabolomics Standards Initiative reporting for chemical analysis (Sumner et al., 2007) and so were not included in the predictive model at this stage. Examples of such compounds include pentahomomethionine (MSI 3) and trihomomethionine (MSI 3), both sulfur-containing amino acids. These were both increased in severe cases and were especially high in patients with a fatal outcome. Other sulfur containing compounds such as cysteine and taurine have been found to be reduced in COVID-19 cases compared to controls, and in COVID-19 patients with moderate-high IL-6 levels (Thomas et al., 2020). Homomethionines such as penta- and tri-homomethionine identified in our results are formed by transamination of oxo-acids that are themselves formed in fatty acid breakdown possibly indicating a procatabolic phenotype, as is common in inflammation (Underwood et al., 2006).

Another compound worthy of further attention is ergothioneine. Ergothioneine is a potent exogenous antioxidant, usually acquired via the consumption of mushrooms (Borodina et al., 2019; Cheah and Halliwell, 2012). The potential protective value in SARS-CoV-2 infections of ergothioneine was recently reviewed by (Cheah and Halliwell, 2020). The results of our study found ergothioneine levels to be following the expected trend, i.e. lower in severe cases and poor outcome; however its *q*-values (in a population whose mushroom consumption was neither monitored nor controlled) fell just slightly short of significance (see Figure S5 A and B). Moreover, piperine (MSI 2) (representative of black pepper consumption) was interestingly found significantly decreased in severe cases and poor outcome (see Figure S5 C and D).

medRxiv preprint doi: https://doi.org/10.1101/2020.12.09.20246389; this version posted December 11, 2020. The copyright holder for this preprint **(which was not certified by peer review)** is the author/funder, who has granted medRxiv a license to display the preprint in perpetuity.

It is made available under a CC-BY-ND 4.0 International license .

This most likely reflects dietary changes in the patients experiencing severe symptoms; however the potential impact of piperine to the host organism is not fully understood.

Limitations and future work

Whilst untargeted LC-MS analysis allows detection of a large number of compounds of diverse chemical classes, limitations in the compound coverage can result from sample preparation methods, LC solvents and gradient. In this study the serum extraction and LC gradient were targeted at hydrophilic compounds, therefore numerous lipids were not reliably measured, i.e. long chain acyl carnitines. Despite this limitation several lipids that exhibit amphiphilic properties e.g. phospholipids and fatty acids were detected and showed significant changes between our patient groups. However, confirmation of their precise identity will require further work before being integrated into a predictive model.

Additional limitations in the presented work come from the preselection of metabolic features that were individually significant in volcano analysis. While this simple method of feature selection narrows the list of compounds it also prevents us from identifying more complex interactions in the case of disjoint populations. More importantly such variable selection performed on all data require validation in a separate patient cohort.

Despite these limitations, multiple significant biological processes were identified as key in discriminating between disease severity and outcome. Future work will aim to validate these findings against a new patient cohort.

Conclusions

We have here performed a well-powered, untargeted metabolomics analysis of serum of COVID-19 patients with the aim of finding prognostic markers of disease severity and outcome. Using both univariate and a multiple predictor Bayesian logistic regression model we found a subset of 20 metabolites with relevant biological functions that are predictive of subsequent disease severity and patient outcome. Although, no individual metabolite appeared be *strongly* discriminative on its own, a combined model based on viral activity, host immune response and underlying metabolic differences showed promising predictive results with AUC 0.792 and 0.793, respectively. These markers hold promise to improve patient care upon COVID-19 infection and diagnosis. Building on these encouraging results, further work will aim to validate those findings and their prognostic potential in a longitudinal study.

medRxiv preprint doi: https://doi.org/10.1101/2020.12.09.20246389; this version posted December 11, 2020. The copyright holder for this preprint **(which was not certified by peer review)** is the author/funder, who has granted medRxiv a license to display the preprint in perpetuity.

It is made available under a CC-BY-ND 4.0 International license .

Methods

Sample acquisition

All samples were acquired at the Royal Liverpool University Hospital (RLUH) on the first positive SARS CoV-2 test (not fasted and different times of the day). Surplus serum was saved after routine diagnostic testing on patients admitted to the hospital who subsequently tested positive for SARS-CoV-2 via PCR. Blood was initially collected into VACUETTE Clot Activator tubes (Greiner, Germany) within approximately 48 h of presentation and centrifuged at 1,500 x *g* for 10 min within 60 min of collection. Surplus serum was stored at –80 ° C prior to processing and analysis. Ethical approval for the use of serum samples and associated metadata in this study was obtained from the local ethics committee (REC ref: 20/NW/0332).

Severity scoring was based on the level of respiratory support required and overall patient outcome where severe = required fraction of inspired oxygen (FIO_2) > 40 % and/or required CPAP and/or required mechanical ventilation and/or did not survive. Patients were also stratified using the 4C Mortality Score (Knight et al., 2020). Patient demographics by severity and outcome are presented in Table 4.

Table 4. **Patient demographics by severity and outcome**. Cohort demographics are presented in counts with percentage (%) of the group total or mean with interquartile range (Q1 – Q3) depending on the data nature. P-values indicating significant differences between groups follow 'star' notation i.e. '***' correspond to p-values <0.001, '**' <0.01, '*' <0.05, '.' < 0.1 and missing when > 0.1. P-values were not calculated for the group counts(N). This study looked at the serum samples from 120 COVID-19 patients. 49 patients developed severe symptoms and 31 patients died as a result of the infection. Severity score metrics based on the 4C Mortality score (Knight et al., 2020) are provided as group means. Some disparity can be observed in gender as women represent 13 % of the severe cases and only 29 % of the deceased patients. Age groups of severe and deceased patients also tend to be slightly higher. BMI do not show significant difference between groups. O_2 support indicates the number of patients that required oxygen support at any time during their hospitalization. Max FiO_2 represent the maximum fraction of inspired oxygen required by the patient during the hospitalization period, where respiratory support capture the patients requiring any support at diagnosis and FiO_2 represents the fraction of inspired oxygen required at time of sample acquisition. As expected, oxygen need and inspired fraction, are highly correlated with severity and fatal outcome. National Early Warning Score (NEWS) also showed correlation with both severity and outcome. Cardiac disease refers to multiple cardiovascular conditions, most frequently: ischemic heart disease, atrial fibrillation, and heart failure. Kidney disease is a grouping of stages G2 to G5 of chronic kidney disease as defined by the National Institute for Health and Care Excellence (NICE) (NICE, 2015). Liver disease in most cases refers to cirrhosis and hepatitis. Malignancy cases vary from lung, bladder, prostate, skin cancer to haematological. Those underlying conditions did not show significance in severity or outcome. Despite kidney disease classification not showing correlation, estimated Glomerular Filtration Rate (eGFR) levels showed significance in severity and outcome. Fever (temperature ≥ 38 °C), cough and Shortness Of Breath (SOB) were noted at time of sample acquisition and did not show relation to severity or outcome. Pulse, systolic Blood Pressure (BP) and respiratory rate also taken at samples acquisition showed correlation with severity and outcome, where higher pulse, higher respiratory rate and lower blood pressure are associated with severe cases and poor outcome. Haemoglobin levels (Hb), white blood cell count (WBC), lymphocyte count (Lymphs), platelets count (PLTs), hematocrit (HCT) and alanine aminotransferase (ALT) measured at sample acquisition did not show significant correlation with severity and outcome. Urea, creatinine, and C-reactive protein (CRP) concentrations are consistently elevated in severe and deceased patients. Hb,WBC, Lymphs, PLTs and HCT were measured on Beckman analyser. ALT, urea, creatinine and CRP were measured on a Roche analyser. Reference ranges are provided in [ ] when available.

medRxiv preprint doi: https://doi.org/10.1101/2020.12.09.20246389; this version posted December 11, 2020. The copyright holder for this preprint (which was not certified by peer review) is the author/funder, who has granted medRxiv a license to display the preprint in perpetuity.

It is made available under a CC-BY-ND 4.0 International license .

Condition	Severity			Outcome		
	Mild	Severe	P-v	Discharged	Deceased	P-v
N	71	49	-	89	31	-
4C score	8.39 (4.75 - 12)	12.87 (10.00 - 16)	***	8.91 (5.25 - 12)	14.34 (13.00 - 16)	***
Male	38 (54%)	32 (65%)		48 (54%)	22 (71%)	.
Female	33 (46%)	17 (35%)		41 (46%)	9 (29%)	.
Age	66.0 (54 - 77)	69.2 (56 - 87)		63.8 (52.0 - 77.0)	77.1 (65.5 - 88.5)	***
BMI	26.4 (21.8 - 28.6)	27.0 (23.0 - 32.0)		26.7 (22.3 - 29.0)	26.4 (21.9 - 29.6)	
O_2 support	32 (45%)	49 (100%)	***	50 (56%)	31 (100%)	***
Max FiO_2	24.7 (21 - 28)	71.6 (40 - 100)	***	33.3 (21 - 35)	74.2 (36 - 100)	***
Respiratory support	17 (24%)	39 (80%)	***	34 (38%)	22 (71%)	**
FiO_2 (%) at dignosis	22.8 (21 - 21)	47.0 (28 - 60)	***	28.2 (21.0 - 28)	45.5 (22.5 - 60)	**
NEWS	2.56 (1 - 4)	7.27 (5 - 10)	***	3.47 (1 - 6.0)	7.40 (6 - 10.8)	***
Hypertension	28 (39%)	26 (53%)		35 (39%)	19 (61%)	*
Cardiac disease	20 (28%)	17 (35%)		25 (28%)	12 (39%)	
Kidney disease	24 (34%)	19 (39%)		28 (31%)	15 (48%)	
eGFR	67.7 (49 - 90)	56.5 (30 - 90)	*	67.7 (48.0 - 90.0)	49.9 (26.5 - 68.5)	**
Liver disease	7 (9.9%)	6 (12.2%)		9 (10%)	4 (13%)	
Malignancy	13 (18%)	6 (12%)		13 (15%)	6 (19%)	
Fever	34 (48%)	30 (61%)		49 (55%)	15 (48%)	
Cough	33 (46%)	29 (59%)		43 (48%)	19 (61%)	
SOB	35 (49%)	29 (59%)		48 (54%)	16 (52%)	
Pulse (BPM)	87.9 (72.0 - 102)	102.8 (91.8 - 114)	***	90.6 (74 - 106)	103.8 (92 - 114)	**
Temp. (°C)	37.1 (36.6 - 37.4)	37.5 (36.7 - 38.1)	*	37.2 (36.6 - 37.5)	37.3 (36.7 - 37.9)	
BP (mmHg)	137 (120 - 151)	123 (102 - 138)	**	135 (120 - 149)	120 (102 - 130)	**
Respiratory rate	20.1 (17 - 22)	26.6 (20 - 30)	***	21.7 (17.0 - 22)	25.7 (19.2 - 30)	*
Hb (g/L) male [133-168] female [118-148]	126 (111 - 141)	124 (107 - 146)		127 (113 - 140)	120 (96 - 146)	
WBC ($x10^9$/L) [3.5-11.0]	8.28 (4.8 - 10.9)	9.98 (5.9 - 11.7)	.	8.63 (5.1 - 11.0)	9.97 (6.5 - 11.6)	
Lymphs ($x10^9$/L) [1.0-3.5]	1.25 (0.75 - 1.4)	1.06 (0.60 - 1.6)		1.239 (0.7 - 1.50)	0.994 (0.5 - 1.35)	.
PLTS ($x10^9$/L) [150-400]	256 (176 - 306)	236 (166 - 292)		255 (175 - 305)	226 (169 - 259)	
HCT (%)	0.372 (0.337 - 0.417)	0.371 (0.329 - 0.436)		0.375 (0.341 - 0.416)	0.361 (0.287 - 0.443)	
ALT (U/L)	32.8 (13 - 31.8)	47.1 (16 - 39.0)		36.1 (15 - 39.0)	46.6 (13 - 31.5)	
Urea (mmol/L)	8.29 (4.6 - 8.75)	13.05 (5.2 - 19.00)	**	8.53 (4.4 - 8.8)	15.12 (8.0 - 22.2)	***
Creatinine (µmol/L)	112 (66 - 104)	133 (70 - 168)		109 (65.0 - 105)	153 (84.5 - 184)	.
CRP (mg/L)	47.7 (11 - 61.2)	132.9 (49 - 190.0)	***	61.4 (13.5 - 79.5)	144.3 (52.5 - 209.5)	***

Sample preparation for metabolomics analysis

Patient serum samples were thawed at room temperature and maintained on ice throughout the sample preparation process. Samples were prepared by addition of 100 µL sample to a 2 mL Eppendorf containing 350 µL Methanol (LC-MS grade) previously cooled at -80 °C and maintained on dry ice whenever possible. The mixture of serum and methanol was vortexed vigorously followed by centrifugation at 18,000 x *g* for 15 min at 4 °C to pellet proteins. Multiple 75 µL aliquots (for extraction replicates) of the resulting supernatant dried in a vacuum centrifuge (ScanVac MaxiVac Beta Vacuum Concentrator system, LaboGene ApS, Denmark) with no temperature application and stored at -80 °C until required for LC-MS/MS analysis.

medRxiv preprint doi: https://doi.org/10.1101/2020.12.09.20246389; this version posted December 11, 2020. The copyright holder for this preprint **(which was not certified by peer review)** is the author/funder, who has granted medRxiv a license to display the preprint in perpetuity.

It is made available under a CC-BY-ND 4.0 International license .

Batch quality controls (QC) and conditioning QC samples were also prepared in this way by pooling serum samples for each batch. Inter-batch quality assurance (IQA) samples were prepared with the same protocol using pooled serum samples provided by RLUH. Therefore, those samples are not representative of the study samples, but representative of the general hospital population and sample acquisition and storage practices.

Additional inter-batch quality assurance samples were prepared using commercial pooled human serum (BioIVT, Lot BRH1413770, Cat: HMSRM, mixed gender 0.1 um filtered) spiked with internal standards. Here, 100 µL sample were added to a 2 mL Eppendorf containing 330 µL Methanol (LC-MS grade) and 20 µL of internal standards mix (ISTDs) as described in (Muelas et al., 2020). The mixture of methanol and internal standards (ISTDs) was previously cooled at -80 °C and maintained on dry ice when adding serum.

Extraction blanks were prepared in the same way as serum samples replacing serum and ISTDs mix with 120 µL of water (LC-MS grade). Prior to analysis, samples were resuspended in 40 µL water (LC-MS), centrifuged at 17,000 x *g* for 15 min at 4 °C to remove any particulates and transferred to glass sample vials.

LC-MS /MS analysis of spent serum samples

Untargeted LC-MS/MS data acquisition was performed as previously described (Muelas et al., 2020) and using published methodologies and guidelines (Broadhurst et al., 2018; Broadhurst and Kell, 2006; Brown et al., 2005 ; Dunn et al., 2011 ; Mullard et al., 2015). Data were acquired using a ThermoFisher Scientific Vanquish UHPLC system coupled to a ThermoFisher Scientific Q-Exactive mass spectrometer (ThermoFisher Scientific, UK).

Samples were analysed following guidelines set out in (Dunn et al., 2011) and (Broadhurst et al., 2018). Briefly, blank extraction samples were injected at the beginning and end of each batch to assess carry over and lack of contamination. QC samples, prepared by pooling equal aliquots of analytical samples in each batch, were applied to condition the analytical platform, enable reproducibility measurements and to correct for systematic errors within batches. Quality Assurance (QA) samples were also incorporated in every batch at regular intervals up to 12 samples per run. Two pools of hospital patient serum (referred as IQA) and commercial serum (referred as SQA) were prepared at the beginning of the study and used in every batch allowing batch alignment in the data processing step. Isotopically labelled internal standards were added to SQA samples, prepared as previously described (Muelas et al., 2020), to monitor mass accuracy. IQA samples were subsequently used to correct across all batches. Four samples per batch were ran with replicates to ensure reproducibility.

LC-MS/MS data preprocessing and analysis

Raw instrument data from all batches in .RAW file format were exported to Compound Discoverer 3.1 (CD3.1) for deconvolution, alignment and annotation (full workflow and settings as described in (Muelas et al., 2020)) based on IQA samples.

Compound grouping was performed in CD3.1 where 6971 compounds in ESI+ and 3122 compounds in ESI- were retained. Retained compounds are selected based on presence in more than 80 % of the IQA, CV less than 30 % and signal 5 times higher than the blank injections. From those compounds 267 in ESI + and 142 in ESI- had identification in mzCloud with score higher than 70 % and full match on Predicted Composition. For all data acquired, annotation and identification criteria were according to (Schymanski et al., 2014) and (Sumner et al., 2007).

Area normalization and batch correction

A custom 2-step normalization was used to correct for small within batch runtime drift and larger between batch variations. This approach showed better results than one step normalization performed by available tools. To perform this, non-normalized peak areas from CD3.1 were exported as a .csv file. QC-based correction was performed in R (version 4.0.2) as discussed in (Dunn et al., 2011) using *fANCOVA* package. The QC correction was performed on each batch independently to remove runtime drift intensity variations.

medRxiv preprint doi: https://doi.org/10.1101/2020.12.09.20246389; this version posted December 11, 2020. The copyright holder for this preprint **(which was not certified by peer review)** is the author/funder, who has granted medRxiv a license to display the preprint in perpetuity.

It is made available under a CC-BY-ND 4.0 International license .

Subsequently, variation between batches was corrected in refence to all batches IQA mean. PCA plots comparing the results for different normalization approaches are included in the supplementary information (Figure S6).

Metadata and multiblock analysis

The following variables in the meta data were used for multivariate analysis: gender, age, BMI, Glasgow coma scale (GCS), NEWS, pulse, temperature, blood pressure, respiratory rate, Hb, WBC, Lymphs, PLTs, HCT, ALT, total bilirubin, urea, creatinine, eGFR, CRP, FiO_2 (%) and O_2 saturation (%) description of the biochemical tests is presented in Table 4. There were 1.44 % missing values in this meta data set and they were imputed by using K-NN imputation algorithm (Troyanskaya et al., 2001).

The multiblock analysis was performed on three data blocks: LC-MS ESI+, ESI- data and metadata. For each block, the data matrix was auto-scaled so that each variable has a mean of 0 and a standard deviation of 1. In addition, a block scaling factor which is the inverse of the square root of the number of variables of this block was applied to compensate differences in variance due the difference in the number of variables. A multiblock PCA (MB-PCA) model called consensus PCA (Smilde et al., 2003) was applied to the three blocks of data. The results of this MB-PCA model are consisted of one super scores matrix which represents the common trend of all the blocks and three block scores matrix which represents the pattern of each block under perspective of the common trend.

Selection of significant metabolic features

Background compounds and compounds detected in less than 25 % of the samples were excluded from the analysis. Compounds were further filtered down based on False Discovery Rate (FDR) corrected *p*-value (i.e. *q*-value) significance < 0.05 and $\log_2$ fold change > 0.5 in severity (i.e. severe vs mild cases) and outcome (i.e. diseased vs discharged patients). *p*-values were calculated using the Mann-Whitney as LC-MS data do not satisfy normality assumption required for T-test. The usually adopted log transformation approach to satisfy T-test requirements tend to overemphasize low abundance compounds; therefore, was not retained in this study.

Significance in severity was detected for 1143/601 compounds in ESI+/-, in outcome 1650/680 ESI+/- made the cut. For simplicity as those two groups tend to overlap the union of the two conditions was taken forward for further analysis 1987/973 ESI+/-.

Signal curation

Significant compounds were manually curated in CD3.1 based on the LC signal quality and MS spectra. LC quality was assessed based on batch retention time (RT) overlap and clear peak separation. MS spectra was evaluated on the detection of preferred ion i.e. $[M+H]^{+1}$ and $[M-H]^{-1}$ with at least 2 isotopes. Additionally, compound where the signal was filled by CD gap fill option for more than 20 % of the QC and 90 % of the samples were also excluded.

Where compounds of interest were detected in both ESI+ and ESI-, the clearest signal was retained for further analysis. When necessary standards were run to confirm MS/MS, RT and signal intensity by polarity. Specifically, in the case of uridine and pseudouridine best separation and signal intensity detection of standards was achieved in ESI-, therefore negative polarity data was used for those compounds.

Pathway enrichment analysis

Pathway enrichment analysis was performed in MUMMICHOG (Li et al., 2013) version 2 incorporated in MetaboAnalyst (Pang et al., 2020). To match the MUMMICHOG requested *m/z* compound format, resolved masses retrieved form CD analysis were altered to achieve $[M+H]^{+1}$ adduct for ESI+ and ESI- results. MUMMICHOG adduct option was set to recognize exclusively $[M+H]^{+1}$ adducts. This allowed processing of ESI+ and ESI- results together and minimize false hits due to multiple adduct matches. Pathways with a high number of significant hits were further manually investigated and hits subsequently verified by MS, RT, MS/MS and match against standards when available.

medRxiv preprint doi: https://doi.org/10.1101/2020.12.09.20246389; this version posted December 11, 2020. The copyright holder for this preprint **(which was not certified by peer review)** is the author/funder, who has granted medRxiv a license to display the preprint in perpetuity.

It is made available under a CC-BY-ND 4.0 International license .

Multiple predictor models

Reported results for multiple predictor models were produced with a Bayesian logistic regression model implemented in R with *rstanarm* R package (Goodrich, 2020). Comparative analysis was performed with the extreme gradient boosting *xgboost* R package (Chen and Guestrin, 2016; Friedman, 2001), Logistic regression with Generalized Linear Models (GLM) *glm* R package and GLM with Elastic net regularization *glmnet* R package (Zou and Hastie, 2005). Data were separated into training and test groups (80:20) with balanced label ratios. Conservative regularization parameters were used to reduce overfitting. Bayesian GLM approach was set to increased regularization with prior scale = 1, for glmnet *alpha* was set to 0.1 and xgboost eta to 0.01 with max_depth = 1. Due to the large group disparities in outcome, weights were incorporated in the model to handle class imbalance. Sparsity inducing parameters such as L1 regularization in glmnet and lasso or hierarchical shrinkage prior in Bayesian GLM were avoided despite better results in some cases. This allowed to perform subgroup selection accounting for compound identity confidence level and known biological role. From the four compared methods Bayesian logistic regression consistently showed better generalization and was therefore retained for results reporting.

Mean and standard deviation for accuracy and AUC were estimated using cross-validation with 100 iterations. These cross-validation results were used to describe the model sensitivity to the data and not for hyperparameters optimization. Visual ROC and 95 % CI representations were obtained from a randomly selected train/test partition using pROC R package with 2000 stratified bootstrap replicates on the test data.

Adjusted compounds significance

Individual OR and 95% CI for selected compounds were evaluated with univariate logistic regression with Generalized Linear Models (glm) implementation in R *stats* package. OR (95 % CI) and *p*-values for significance are presented in the reported tables. Compounds are adjusted for age, gender, BMI, liver disease, cardiovascular disease, hypertension, kidney disease (i.e. chronic kidney disease stages 2 to 5), diabetes mellitus (type 1 or 2) and all together. Liver conditions include cirrhosis, hepatitis, alcoholic hepititis, autoimmune hepatitis, ascites, transplant, fatty liver disease. Cardiovascular conditons include ischaemic heart disease (IHD), atrial fibrillation (AF), cardiomegaly, cardiomyopathy, left ventricular systolic dysfunction, left ventricular hypertrophy, left ventricular failure, congestive heart failure, drug induced myocarditis, heart failure, angina and Takotsubo cardiomyopathy with IHD and AF being most frequent.

medRxiv preprint doi: https://doi.org/10.1101/2020.12.09.20246389; this version posted December 11, 2020. The copyright holder for this preprint **(which was not certified by peer review)** is the author/funder, who has granted medRxiv a license to display the preprint in perpetuity.

It is made available under a CC-BY-ND 4.0 International license .

Acknowledgements

We thank the UK BBSRC (grant BB/V003976/1) and the Novo Nordisk Foundation (grant NNF10CC1016517) for financial support.

Contributions

D.B.K. and R.G. conceived the study and obtained funding for grant to enable this work.

A.S.D and J.M.T. obtained ethical approval, acquired samples and metadata.

A.S. created data base to store data.

M.W.M. and I.R. designed LC-MS/MS acquisition with advice from Y.X., D.B.K. and R. G.

M.W.M., J.M.G. and N.G. prepared samples and performed LC-MS/MS acquisition

M.W.M and I.R. processed data. I.R. performed data analysis, with Multi-block analysis performed by Y.X.

M.W.M. and I.R. performed data interpretation and wrote the manuscript with D.B.K.

ALL authors read and approve of the final version of the manuscript.

Conflict of interest

All authors declare that they have no conflict of interest.

medRxiv preprint doi: https://doi.org/10.1101/2020.12.09.20246389; this version posted December 11, 2020. The copyright holder for this preprint **(which was not certified by peer review)** is the author/funder, who has granted medRxiv a license to display the preprint in perpetuity.

It is made available under a CC-BY-ND 4.0 International license .

References

Anderson, S.G., Dunn, W.B., Banerjee, M., Brown, M., Broadhurst, D.I., Goodacre, R., Cooper, G.J.S., Kell, D.B., and Cruickshank, J.K. (2014). Evidence That Multiple Defects in Lipid Regulation Occur before Hyperglycemia during the Prodrome of Type-2 Diabetes. PLOS ONE *9*, e103217.

Arunachalam, P.S., Wimmers, F., Mok, C.K.P., Perera, R.A.P.M., Scott, M., Hagan, T., Sigal, N., Feng, Y., Bristow, L., Tak-Yin Tsang, O.*, et al.* (2020). Systems biological assessment of immunity to mild versus severe COVID-19 infection in humans. Science *369*, 1210.

Bennet, B.M., Wolf, J., Laureano, R., and Sellers, R.S. (2020). Review of Current Vaccine Development Strategies to Prevent Coronavirus Disease 2019 (COVID-19). Toxicol Pathol, 192623320959090.

Blasco, H., Bessy, C., Plantier, L., Lefevre, A., Piver, E., Bernard, L., Marlet, J., Stefic, K., Benz-de Bretagne, I., Cannet, P.*, et al.* (2020). The specific metabolome profiling of patients infected by SARS-COV-2 supports the key role of tryptophan-nicotinamide pathway and cytosine metabolism. Scientific Reports *10*, 16824.

Blaženović, I., Kind, T., Ji, J., and Fiehn, O. (2018). Software tools and approaches for compound identification of LC-MS/MS data in metabolomics. Metabolites *8*, 31.

Borodina, I., Kenny, L.C., McCarthy, C.M., Paramasivan, K., Pretorius, E., Roberts, T.J., van der Hoek, S.A., and Kell, D.B. (2019). The biology of ergothioneine, an antioxidant nutraceutical. Nutrition Research Reviews, 1-28.

Broadhurst, D., Goodacre, R., Reinke, S.N., Kuligowski, J., Wilson, I.D., Lewis, M.R., and Dunn, W.B. (2018). Guidelines and considerations for the use of system suitability and quality control samples in mass spectrometry assays applied in untargeted clinical metabolomic studies. Metabolomics *14*, 72.

Broadhurst, D.I., and Kell, D.B. (2006). Statistical strategies for avoiding false discoveries in metabolomics and related experiments. Metabolomics *2*, 171-196.

Brown, M., Dunn, W.B., Ellis, D.I., Goodacre, R., Handl, J., Knowles, J.D., O'Hagan, S., Spasić, I., and Kell, D.B. (2005). A metabolome pipeline: from concept to data to knowledge. Metabolomics *1*, 39-51.

Cheah, I.K., and Halliwell, B. (2012). Ergothioneine; antioxidant potential, physiological function and role in disease. Biochimica et Biophysica Acta (BBA)-Molecular Basis of Disease *1822*, 784-793.

Cheah, I.K., and Halliwell, B. (2020). Could Ergothioneine Aid in the Treatment of Coronavirus Patients? Antioxidants *9*, 595.

Chen, T., and Guestrin, C. (2016). Xgboost: A scalable tree boosting system. Paper presented at: Proceedings of the 22nd acm sigkdd international conference on knowledge discovery and data mining.

Danchin, A., and Marlière, P. (2020). Cytosine drives evolution of SARS-CoV-2. Environmental Microbiology *22*, 1977-1985.

Dunn, W.B., Broadhurst, D., Begley, P., Zelena, E., Francis-McIntyre, S., Anderson, N., Brown, M., Knowles, J.D., Halsall, A., Haselden, J.N.*, et al.* (2011). Procedures for large-scale metabolic profiling of serum and plasma using gas chromatography and liquid chromatography coupled to mass spectrometry. Nat Protoc *6*, 1060-1083.

Dunn, W.B., Broadhurst, D.I., Deepak, S.M., Buch, M.H., McDowell, G., Spasic, I., Ellis, D.I., Brooks, N., Kell, D.B., and Neyses, L. (2007). Serum metabolomics reveals many novel metabolic markers of heart failure, including pseudouridine and 2-oxoglutarate. Metabolomics *3*, 413-426.

Dunn, W.B., Lin, W., Broadhurst, D., Begley, P., Brown, M., Zelena, E., Vaughan, A.A., Halsall, A., Harding, N., and Knowles, J.D. (2015). Molecular phenotyping of a UK population: defining the human serum metabolome. Metabolomics *11*, 9-26.

medRxiv preprint doi: https://doi.org/10.1101/2020.12.09.20246389; this version posted December 11, 2020. The copyright holder for this preprint **(which was not certified by peer review)** is the author/funder, who has granted medRxiv a license to display the preprint in perpetuity.

It is made available under a CC-BY-ND 4.0 International license .

Fox, S.E., Akmatbekov, A., Harbert, J.L., Li, G., Quincy Brown, J., and Vander Heide, R.S. (2020). Pulmonary and cardiac pathology in African American patients with COVID-19: an autopsy series from New Orleans. The Lancet Respiratory Medicine *8*, 681-686.

Friedman, J.H. (2001). Greedy function approximation: a gradient boosting machine. Annals of statistics, 1189-1232.

Goodrich, B. (2020). rstanarm: Bayesian applied regression modeling via Stan., I.A. Jonah Gabry, Sam Brilleman, ed.

Grobler, C., Maphumulo, S.C., Grobbelaar, L.M., Bredenkamp, J.C., Laubscher, G.J., Lourens, P.J., Steenkamp, J., Kell, D.B., and Pretorius, E. (2020). Covid-19: the rollercoaster of fibrin (Ogen), D-dimer, Von Willebrand factor, P-Selectin and their interactions with endothelial cells, platelets and erythrocytes. International Journal of Molecular Sciences *21*, 5168.

Guo, H., Chou, W.-C., Lai, Y., Liang, K., Tam, J.W., Brickey, W.J., Chen, L., Montgomery, N.D., Li, X., and Bohannon, L.M. (2020). Multi-omics analyses of radiation survivors identify radioprotective microbes and metabolites. Science *370*.

Hadjadj, J., Yatim, N., Barnabei, L., Corneau, A., Boussier, J., Smith, N., Péré, H., Charbit, B., Bondet, V., Chenevier-Gobeaux, C.*, et al.* (2020). Impaired type I interferon activity and inflammatory responses in severe COVID-19 patients. Science *369*, 718.

Huang, C.-F., Cheng, M.-L., Fan, C.-M., Hong, C.-Y., and Shiao, M.-S. (2013). Nicotinuric Acid. Diabetes Care *36*, 1729.

Hunt, B.C., e Cordeiro, T.M., Robert, S., de Dios, C., Leal, V.A.C., Soares, J.C., Robert, D., Antonio, T., and Sudhakar, S.M. (2020). Effect of mmune Activation on the Kynurenine Pathway and Depression Symptoms–A Systematic Review and Meta-Analysis. Neuroscience & Biobehavioral Reviews.

Hussain, A., Mahawar, K., Xia, Z., Yang, W., and Shamsi, E.-H. (2020). Obesity and mortality of COVID-19. Meta-analysis. Obesity research & clinical practice.

Iaccarino, G., Grassi, G., Borghi, C., Ferri, C., Salvetti, M., and Volpe, M. (2020). Age and multimorbidity predict death among COVID-19 patients: results of the SARS-RAS study of the Italian Society of hypertension. Hypertension *76*, 366-372.

Kell, D.B., and Goodacre, R. (2014). Metabolomics and systems pharmacology: why and how to model the human metabolic network for drug discovery. Drug Discovery Today *19*, 171-182.

Kell, D.B., and Oliver, S.G. (2016). The metabolome 18 years on: a concept comes of age. Metabolomics *12*, 148.

Kell, D.B., and Westerhoff, H.V. (1986). Metabolic control theory: its role in microbiology and biotechnology. FEMS Microbiology Letters *39*, 305-320.

Kenny, L.C., Broadhurst, D.I., Dunn, W., Brown, M., North, R.A., McCowan, L., Roberts, C., Cooper, G.J., Kell, D.B., and Baker, P.N. (2010). Robust early pregnancy prediction of later preeclampsia using metabolomic biomarkers. Hypertension *56*, 741-749.

Kim, M., Jung, S., Lee, S.-H., and Lee, J.H. (2015). Association between Arterial Stiffness and Serum L-Octanoylcarnitine and Lactosylceramide in Overweight Middle-Aged Subjects: 3-Year Follow-Up Study. PLOS ONE *10*, e0119519.

Kimhofer, T., Lodge, S., Whiley, L., Gray, N., Loo, R.L., Lawler, N.G., Nitschke, P., Bong, S.-H., Morrison, D.L., Begum, S.*, et al.* (2020). Integrative Modelling of Quantitative Plasma Lipoprotein, Metabolic and Amino Acid Data Reveals a Multi-organ Pathological Signature of SARS-CoV-2 Infection. Journal of Proteome Research.

Knight, S.R., Ho, A., Pius, R., Buchan, I., Carson, G., Drake, T.M., Dunning, J., Fairfield, C.J., Gamble, C., Green, C.A.*, et al.* (2020). Risk stratification of patients admitted to hospital with covid-19 using the ISARIC WHO Clinical Characterisation Protocol: development and validation of the 4C Mortality Score. BMJ *370*, m3339.

Leisman, D.E., Deutschman, C.S., and Legrand, M. (2020). Facing COVID-19 in the ICU: vascular dysfunction, thrombosis, and dysregulated inflammation. Intensive Care Medicine *46*, 1105-1108.

medRxiv preprint doi: https://doi.org/10.1101/2020.12.09.20246389; this version posted December 11, 2020. The copyright holder for this preprint **(which was not certified by peer review)** is the author/funder, who has granted medRxiv a license to display the preprint in perpetuity.

It is made available under a CC-BY-ND 4.0 International license .

Li, S., Park, Y., Duraisingham, S., Strobel, F.H., Khan, N., Soltow, Q.A., Jones, D.P., and Pulendran, B. (2013). Predicting network activity from high throughput metabolomics. PLoS Comput Biol *9*, e1003123.

Li, Y., Hu, N., Yang, D., Oxenkrug, G., and Yang, Q. (2017). Regulating the balance between the kynurenine and serotonin pathways of tryptophan metabolism. The FEBS journal *284*, 948-966.

Libby, P., and Lüscher, T. (2020). COVID-19 is, in the end, an endothelial disease. European Heart Journal *41*, 3038-3044.

Marietta, M., Ageno, W., Artoni, A., De Candia, E., Gresele, P., Marchetti, M., Marcucci, R., and Tripodi, A. (2020). COVID-19 and haemostasis: a position paper from Italian Society on Thrombosis and Haemostasis (SISET). Blood Transfus *18*, 167-169.

Migaud, M., Gandotra, S., Chand, H.S., Gillespie, M.N., Thannickal, V.J., and Langley, R.J. (2020). Metabolomics to Predict Antiviral Drug Efficacy in COVID-19. American Journal of Respiratory Cell and Molecular Biology *63*, 396-398.

Muelas, M.W., Roberts, I., Mughal, F., O'Hagan, S., Day, P.J., and Kell, D.B. (2020). An untargeted metabolomics strategy to measure differences in metabolite uptake and excretion by mammalian cell lines. bioRxiv, 2020.2006.2002.129239.

Mullard, G., Allwood, J.W., Weber, R., Brown, M., Begley, P., Hollywood, K.A., Jones, M., Unwin, R.D., Bishop, P.N., Cooper, G.J.S.*, et al.* (2015). A new strategy for MS/MS data acquisition applying multiple data dependent experiments on Orbitrap mass spectrometers in non-targeted metabolomic applications. Metabolomics *11*, 1068-1080.

Murray, M.F. (2003). Nicotinamide: An Oral Antimicrobial Agent with Activity against Both Mycobacterium tuberculosis and Human Immunodeficiency Virus. Clinical Infectious Diseases *36*, 453-460.

Nakano, K., Nakao, T., Schram, K.H., Hammargren, W.M., McClure, T.D., Katz, M., and Petersen, E. (1993). Urinary excretion of modified nucleosides as biological marker of RNA turnover in patients with cancer and AIDS. Clinica chimica acta *218*, 169-183.

NICE (2015). Chronic kidney disease in adults: assessment and management. NICE *Clinical guideline [CG182]*.

Oliver, S.G., Winson, M.K., Kell, D.B., and Baganz, F. (1998). Systematic functional analysis of the yeast genome. Trends in biotechnology *16*, 373-378.

Ottosson, F., Smith, E., Melander, O., and Fernandez, C. (2018). Altered asparagine and glutamate homeostasis precede coronary artery disease and type 2 diabetes. The Journal of Clinical Endocrinology & Metabolism *103*, 3060-3069.

Overmyer, K.A., Shishkova, E., Miller, I.J., Balnis, J., Bernstein, M.N., Peters-Clarke, T.M., Meyer, J.G., Quan, Q., Muehlbauer, L.K., and Trujillo, E.A. (2020). Large-Scale Multi-omic Analysis of COVID-19 Severity. Cell systems.

Pang, Z., Chong, J., Li, S., and Xia, J. (2020). MetaboAnalystR 3.0: Toward an Optimized Workflow for Global Metabolomics. Metabolites *10*, 186.

Paranjpe, I., Fuster, V., Lala, A., Russak, A.J., Glicksberg, B.S., Levin, M.A., Charney, A.W., Narula, J., Fayad, Z.A., Bagiella, E.*, et al.* (2020). Association of Treatment Dose Anticoagulation With In-Hospital Survival Among Hospitalized Patients With COVID-19. Journal of the American College of Cardiology *76*, 122-124.

Pretorius, E., Venter, C., Laubscher, G.J., Lourens, P.J., Steenkamp, J., and Kell, D.B. (2020). Prevalence of amyloid blood clots in COVID-19 plasma. medRxiv, 2020.2007.2028.20163543.

Raamsdonk, L.M., Teusink, B., Broadhurst, D., Zhang, N., Hayes, A., Walsh, M.C., Berden, J.A., Brindle, K.M., Kell, D.B., and Rowland, J.J. (2001). A functional genomics strategy that uses metabolome data to reveal the phenotype of silent mutations. Nature biotechnology *19*, 45-50.

Rattray, N.J.W., Trivedi, D.K., Xu, Y., Chandola, T., Johnson, C.H., Marshall, A.D., Mekli, K., Rattray, Z., Tampubolon, G., Vanhoutte, B.*, et al.* (2019). Metabolic dysregulation in vitamin E and carnitine shuttle energy mechanisms associate with human frailty. Nature Communications *10*, 5027.

medRxiv preprint doi: https://doi.org/10.1101/2020.12.09.20246389; this version posted December 11, 2020. The copyright holder for this preprint **(which was not certified by peer review)** is the author/funder, who has granted medRxiv a license to display the preprint in perpetuity.

It is made available under a CC-BY-ND 4.0 International license .

Salek, R.M., Steinbeck, C., Viant, M.R., Goodacre, R., and Dunn, W.B. (2013). The role of reporting standards for metabolite annotation and identification in metabolomic studies. GigaScience *2*, 2047-2217X-2042-2013.

Schymanski, E.L., Jeon, J., Gulde, R., Fenner, K., Ruff, M., Singer, H.P., and Hollender, J. (2014). Identifying Small Molecules via High Resolution Mass Spectrometry: Communicating Confidence. Environmental Science & Technology *48*, 2097-2098.

Shen, B., Yi, X., Sun, Y., Bi, X., Du, J., Zhang, C., Quan, S., Zhang, F., Sun, R., Qian, L.*, et al.* (2020). Proteomic and Metabolomic Characterization of COVID-19 Patient Sera. Cell *182*, 59-72.e15.

Smilde, A.K., van der Werf, M.J., Bijlsma, S., van der Werff-van der Vat, B.J., and Jellema, R.H. (2005). Fusion of mass spectrometry-based metabolomics data. Analytical chemistry *77*, 6729-6736.

Smilde, A.K., Westerhuis, J.A., and de Jong, S. (2003). A framework for sequential multiblock component methods. Journal of Chemometrics: A Journal of the Chemometrics Society *17*, 323-337.

Sumner, L.W., Amberg, A., Barrett, D., Beale, M.H., Beger, R., Daykin, C.A., Fan, T.W.M., Fiehn, O., Goodacre, R., Griffin, J.L.*, et al.* (2007). Proposed minimum reporting standards for chemical analysis. Metabolomics *3*, 211-221.

Thaker, S.K., Ch'ng, J., and Christofk, H.R. (2019). Viral hijacking of cellular metabolism. BMC Biology *17*, 59.

Thomas, T., Stefanoni, D., Reisz, J.A., Nemkov, T., Bertolone, L., Francis, R.O., Hudson, K.E., Zimring, J.C., Hansen, K.C., Hod, E.A.*, et al.* (2020). COVID-19 infection alters kynurenine and fatty acid metabolism, correlating with IL-6 levels and renal status. JCI Insight *5*.

Trivedi, D.K., Hollywood, K.A., and Goodacre, R. (2017). Metabolomics for the masses: The future of metabolomics in a personalized world. New horizons in translational medicine *3*, 294-305.

Troyanskaya, O., Cantor, M., Sherlock, G., Brown, P., Hastie, T., Tibshirani, R., Botstein, D., and Altman, R.B. (2001). Missing value estimation methods for DNA microarrays. Bioinformatics *17*, 520-525.

Underwood, B.R., Broadhurst, D., Dunn, W.B., Ellis, D.I., Michell, A.W., Vacher, C., Mosedale, D.E., Kell, D.B., Barker, R.A., and Grainger, D.J. (2006). Huntington disease patients and transgenic mice have similar pro-catabolic serum metabolite profiles. Brain *129*, 877-886.

Wu, Z., and McGoogan, J.M. (2020). Characteristics of and Important Lessons From the Coronavirus Disease 2019 (COVID-19) Outbreak in China: Summary of a Report of 72314 Cases From the Chinese Center for Disease Control and Prevention. JAMA *323*, 1239-1242.

Wynants, L., Van Calster, B., Collins, G.S., Riley, R.D., Heinze, G., Schuit, E., Bonten, M.M.J., Dahly, D.L., Damen, J.A.A., Debray, T.P.A.*, et al.* (2020). Prediction models for diagnosis and prognosis of covid-19: systematic review and critical appraisal. BMJ *369*, m1328.

Xu, Y., and Goodacre, R. (2012). Multiblock principal component analysis: an efficient tool for analyzing metabolomics data which contain two influential factors. Metabolomics *8*, 37-51.

Zhang, Q., Bastard, P., Liu, Z., Le Pen, J., Moncada-Velez, M., Chen, J., Ogishi, M., Sabli, I.K.D., Hodeib, S., Korol, C.*, et al.* (2020). Inborn errors of type I IFN immunity in patients with life-threatening COVID-19. Science *370*, eabd4570.

Zheng, Y.-Y., Ma, Y.-T., Zhang, J.-Y., and Xie, X. (2020). COVID-19 and the cardiovascular system. Nature Reviews Cardiology *17*, 259-260.

Zou, H., and Hastie, T. (2005). Regularization and variable selection via the elastic net. Journal of the Royal Statistical Society: Series B (Statistical Methodology) *67*, 301-320.